01 Oct 1965

Strength of three new types of composite beams

A. A. Toprac

BULLETIN No. 2, OCTOBER, 1965 *Toprac* – STRENGTH OF THREE NEW TYPES OF COMPOSITE BEAMS

STEEL RESEARCH for construction

STRENGTH OF THREE NEW TYPES OF COMPOSITE BEAMS *by A. A. Toprac*

Committee of Steel Plate Producers

american iron and steel institute

BULLETIN No. 2, OCTOBER, 1965

STRENGTH OF THREE NEW TYPES OF COMPOSITE BEAMS

By

A. A. TOPRAC

PART I

Part I of this report is reprinted from the AISC Engineering Journal, Jan., 1965, Vol. 2. No. 1.

Strength of Three New Types of Composite Beams

A. A. TOPRAC

ALTHOUGH COMPOSITE construction is not new, having been in use in this country since the late 1930's, it owes its current popularity in building construction to relatively recent developments. Since the advantages of composite construction—reduced weight of steel, smaller live load deflection, or decreased depth of members—are most pronounced in long spans and for heavy loads, most of the early work was done in the bridge field. However, neither the original nor the revised provisions on composite construction in the specifications of the American Association of State Highway Officials (AASHO)[1], which were written specifically for bridges, were directly applicable to building construction because of the different nature of the problems involved.

The 1961 and 1963 revisions of the American Institute of Steel Construction (AISC) Specification[2] stimulated composite design for buildings by including provisions for composite beams without encasement as well as the old requirements of 1946 for fully encased beams. Until 1961 there was no applicable specification which included the practical and proven developments of that time. The sections of the above specification dealing with this subject are based on the recommendations of the ASCE-ACI Joint Committee published in 1960[3] and an experimental investigation completed at Lehigh University in 1961.[4, 5]

The development of the headed stud shear connector in the 1950's has accelerated the acceptance of composite construction by alleviating many of the fabrication and handling problems inherent with older types of shear connectors such as the channel and the spiral.[6]

The 1963 AISC Specification allows the use of high strength steels conforming to American Society for Testing and Materials (ASTM) Specifications A242, A440 and A441. The yield requirements for the three high strength grades are the same, and decrease from 50,000 to 42,000 psi as the thickness of the material increases. In practice, construction steels with yield strengths up to 100,000 psi are available. The strongest are the quenched and tempered alloy steels having yield strengths in the range of 90,000 to 100,000 psi. These constructional alloy steels are covered by ASTM A514 Specification.

In traditional steel framing, particularly for building construction, deflection and/or buckling considerations often limit the application of higher strength steels. In composite construction these limitations are minimized or reduced and full advantage may be taken of the higher strength steels. In a recent study of hybrid steel girders[7] composed of constructional alloy steel flanges and A36 steel web, the authors state:

> Both the lateral buckling problem and the deflection problem encountered through the use of high-strength steel flanges can be resolved by using composite construction. The use of this method of construction not only furnishes lateral support for the compression flange, but also increases the moment of inertia of the section so that it will not deflect as much. Since the stress in the compression flange of a composite section is usually quite low, this flange would not need to be composed of high strength steel. The use of composite construction seems to offer the most possibilities for the efficient use of high strength steel and carbon steel combinations.

TEST PROGRAM

The investigation reported in this paper was a pilot study into three relatively unexplored areas of composite design in steel and concrete. The three areas were: (a) the use of raised patterned floor plate as a shear transfer device, (b) composite hybrid steel sections with high strength bottom flanges, and (c) composite beams with inverted steel T sections (top steel flange omitted). The purpose of the investigation was to obtain data on the structural behavior of the three types of beams subjected to static loading.

In order to achieve the above-mentioned objective, a test program of seventeen beams was designed as outlined in Table 1. There were four groups of specimens, called Series 1 to 4. For each series, the object of the investigation, the steel profile, the types of steel used and the designations of specimens are shown in Table 1.

A. A. Toprac is Professor of Civil Engineering, The University of Texas, Austin, Tex., and is a Professional Member of AISC.

Table 1. Outline of Experimental Program

Series Number	Object of Investigation	Steel Sections				Specimens
		Profile	Types of Steel[b]			
			Top Flange	Web	Bottom Flange	
1	Floor plate for top flange	Unsymmetrical I	Floor Pl.	A36	A36	12, 14a, 14b, 15
		Unsymmetrical I	A36	A36	A36	11
		Symmetrical I	Floor Pl.	A36	A36	13
2	Hybrid steel section	Symmetrical I	A36	A36	A36	21
		Symmetrical I	A36	A36	H.S.S.[a]	22a, 22b, 23
3	Hybrid steel section	Symmetrical I	A36	A36, H.S.S.[a]	H.S.S.[a]	32, 33a, 33b, 34, 35
4	Steel section without top flange	Inverted tee	None	A36	A36	41a, 41b

[a] *H.S.S. = High strength steel, either A441 or A514.*
[b] *Cross-sectional area of the steel section was the same in all specimens.*

Table 1a. Static Yield Strength of Steel Plates

Type of Material	Plate Thickness, in.	Average Static Yield Points, ksi
A36	½	33.4; 33.0
A36	¼	35.2
Floor Pl.	½	42.7
A441	½	53.0
A441	¼	51.2
A514	½	110.6
A514	¼	106[a]

[a] *For Beam 35 the lower web plate yield strength of 150 ksi is not included in this average.*

The cross-sections of the specimens and the loading arrangement are shown in Fig. 1. All specimens were designed to have the same depth of steel section, concrete flange, area of steel, and thickness of flange and web plates, and were tested with the same loading arrangement.

The steel sections were fabricated from A36, A441, A514 and floor steel plates; the combinations of materials used are shown in Fig. 2. The average static yield points for the steel used in the beams are shown in Table 1a. The slabs were made with river gravel and sand concrete having average cylinder strengths of 3,840 psi. They were reinforced with 0.2 percent of longitudinal steel and 0.62 percent of transverse steel. The steel sections and the concrete slabs were interconnected with headed stud shear connectors of ½ or ⅜-in. diameter. The number, size and spacing of studs used in each beam are given in Table 2. The last column in Table 2 compares the furnished shear connectors with those that would be required by the AISC Specification.[2]

The load was applied in steps of varying magnitude in such a manner that the deflections of the specimen were never allowed to decrease. All tests were continued past the ultimate load and were usually discontinued after the load had dropped off substantially from the ultimate. Deflection and end slip between the steel section and the concrete slab were measured at every load increment in all tests. In addition, strain measurements were made in the shear span and at the center line of beams 32 and 33b by means of electric resistance strain gages.

Further details on specimens, materials, and testing procedures are given in Part II of Reference 8.

NOMENCLATURE

a = depth of concrete stress block
b = width of concrete compression flange
C = total compressive force in the composite section
c' = compressive force in concrete flange of a composite beam with inadequate shear connectors
c'' = compressive force in the steel section of a composite beam with inadequate shear connectors
d = total depth of composite section
e = moment arm between resultant compression and tension forces at M_u
f_c' = cylinder strength of concrete at the age of testing
f_y = static yield point of steel
M = applied moment = 3.25 × P
M_m = maximum applied moment (includes dead load of 7.1 ft-kips)
M_p = theoretical plastic moment capacity of the steel section alone
M_{ps} = total theoretical ultimate resisting moment of the concrete slab and steel section acting together but without composite action
M_u = theoretical ultimate moment of a composite section with adequate shear connectors

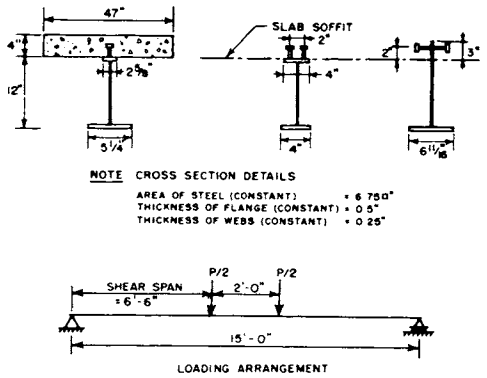

Fig. 1. Description of specimens and tests

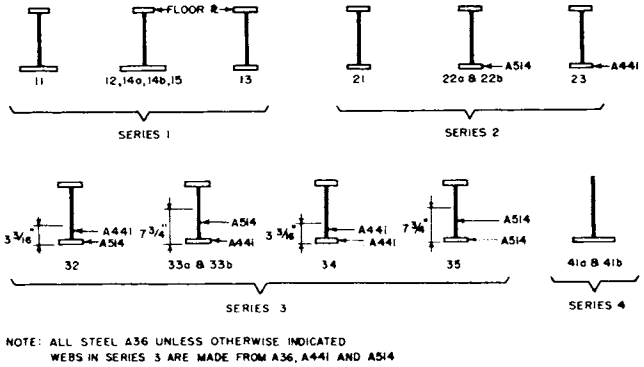

Fig. 2. Steel sections

M_u' = theoretical ultimate moment of a composite section with inadequate shear connectors
M_y = theoretical yield moment of a composite section based on first yield at any point in the beam
P = externally applied load
q_u = the ultimate shear strength of a shear connector
T = total tensile force in the composite section

TEST RESULTS AND DISCUSSION

The general modes of failure observed during the testing of composite beams of this program are discussed below. The structural behavior of each beam is presented and maximum carrying capacities, deflections and slips are given. Where applicable, comparisons are made between beams and between series. The test data and certain additional analytical studies are presented in Part II of Reference 8.

General Modes of Failure—All beams in this test program failed in one of three modes which will be described as: (1) flexural failure, (2) shear failure in the studs and (3) shear failure in the concrete slab.

Flexural failure of a composite section occurs when the slab compressive stresses are brought to the ultimate by bending, resulting in crushing of the concrete followed by a major loss of moment capacity. Figure 3 is a photograph of such a concrete failure in specimen 22a. Similar failure is shown in Fig. 4, which is a photograph of specimen 12 taken after it was removed from the testing machine. This type of failure implies that the shear connection was adequate. For the specimens of this

Table 2. Shear Connectors

Specimen Number[a]	Size of Shear Connectors	No. of Connectors per Shear Span[b]	Spacing of Connectors in Shear Span, in.	Percent of AISC Requirements
11	½ in. dia. × 3 in.	24	3¼	100
12	"	16	4¾	67
13	"	7	10	29
14a	"	7	10	29
14b	"	7	10	29
15	"	4	20	17
21	½ in. dia. × 3 in.	24	6½	100
22a	"	26	6	72
22b	"	26	6	72
23	"	36	4¼	138
32	½ in. dia. × 3 in.	28	5½	74
33a	"	48	4	126
33b	"	48	4	126
34	"	28	5½	100
35	"	48	4	100
41a	⅜ in. dia. × 3 in.	58	2¾	—
41b	"	58	2¾	—

[a] *Letters* a *and* b *distinguish between two duplicate specimens.*
[b] *In addition to the studs in the two shear spans, two studs were placed at or near the midspan of each beam.*

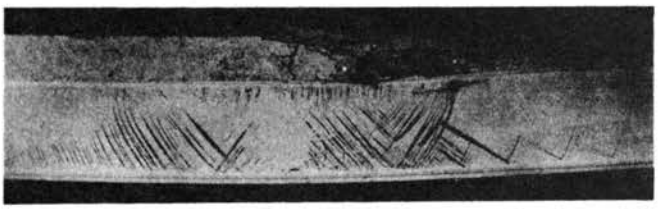

Fig. 3. Picture of Beam 22a at the end of the test. Note the crushing of the concrete slab (flexural failure). The whole steel section was yielded in tension just before the concrete crushed. The typical compression type yield lines at the upper part of the web occurred after the crushing of the concrete when the beam started carrying loads independently.

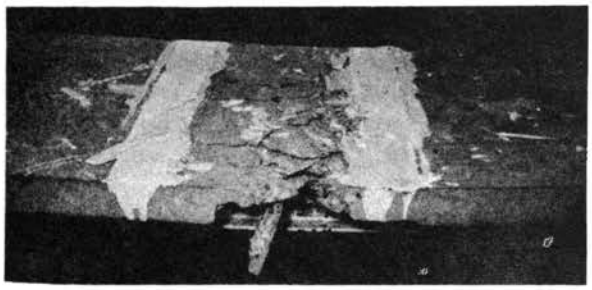

Fig. 4. Beam 12 after removal from testing machine. Photo shows typical top view of specimens which failed in flexure.

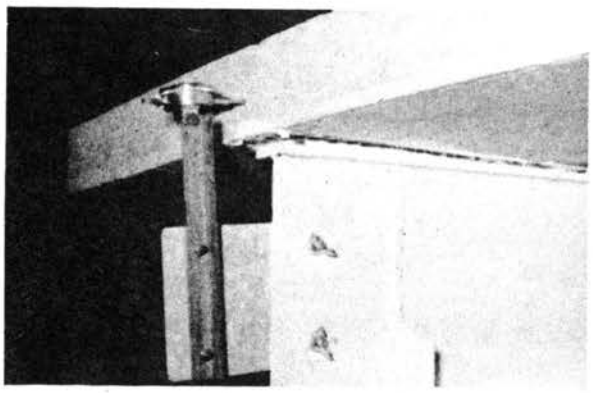

Fig. 5. Beam 14b at failure. Note the large slip between the steel flange and the concrete slab. Also the separation between steel and concrete can be clearly seen.

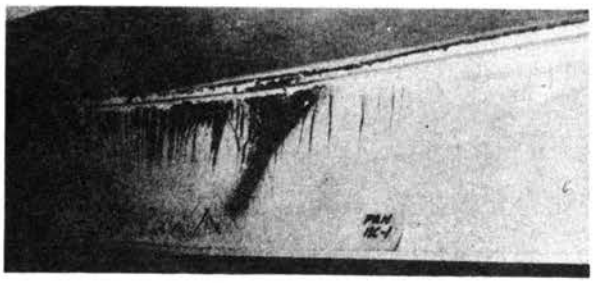

Fig. 6. View of Beam 14b before removal from testing machine. Note the slip and separation between steel shape and concrete slab. The deep compression-type yield lines occurred after the shear failure took place and the steel beam flange buckled laterally while the web buckled locally. The absence of tension yield lines above the middle of the web is apparent. The beam did not reach its calculated M_u.

program, in which the neutral axis was well above the steel section at ultimate moment, flexural failure was similar to the tension failure of an under-reinforced concrete beam. As yielding of the steel section progressed, the neutral axis rose until the compression stresses in the extreme fibers of the concrete became critical. This is the most desirable mode of failure for steel-concrete beams, since it allows the cross-section to mobilize all of its resistance and failure occurs only after considerable deflection and cracking.

Most of the beams tested in this program, following a flexural failure at their maximum moment value, were able to maintain moments which were of higher magnitude than the plastic moment value M_p of the steel section alone. This indicated that part of the concrete slab, although considerably damaged, was still available to help carry the loads, or that the strains in the steel section reached strain hardening at places where the slab was ineffective. Most of the beams exhibited remarkable reserve strength after the crushing of the concrete flange. The post-failure strength was limited by buckling of the steel section. Following the flexural failure of the composite section, the concrete slab could not provide effective lateral support in the constant moment region. Thus the steel section usually buckled either laterally or in the web.

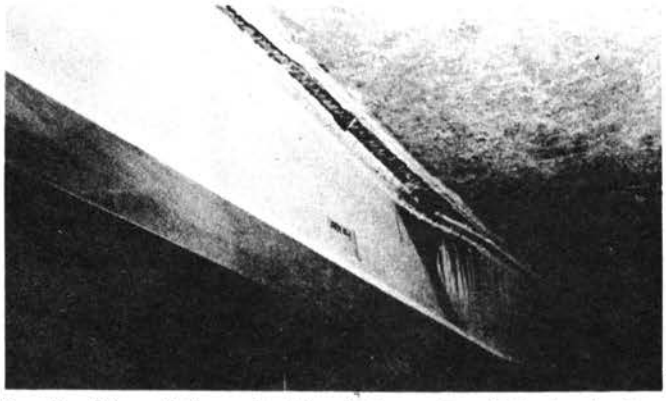

Fig. 7. View of the underside of Beam 15 which clearly shows: (a) the absence of tension type yield lines, (b) the separation between steel and concrete (c) the flange and web buckling with the accompanying compression yielding.

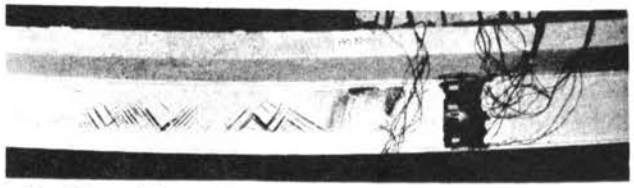

Fig. 8. View of Beam 32 at the end of the test. The separation at the right end and the absence of concrete crushing at midspan can be noted. This is a typical view of specimens with shear failure. The A514 portion of the web shows no yield lines. Web buckled after the maximum load was reached. Yielding due to buckling can also be seen.

Shear failure of a composite beam occurred when the shear connection was inadequate. Specimens which failed in this manner sheared off all studs in one of the shear spans and allowed the slab to separate and slip grossly, thus resulting in a major decrease in moment resistance due to the loss of composite action. After failure of the studs, the slab cracked transversely just outside one of the loads. At this point, with the studs broken, there was only friction available to provide lateral support and the steel section was relatively free to buckle. For all specimens which exhibited shear failure, the steel section was able to develop moment close to its M_p value before buckling caused the test to be stopped. Figures 5, 6, 7 and 8 are photographs which show failures of this type in specimens 14b, 15, and 32. The separation of steel and concrete is visible in all these pictures.

Only one beam, 41a, suffered a shear failure in the concrete slab. This particular beam failure will be discussed in greater detail with the results of Series 4.

Series 1—The objective of this series was to determine whether the use of the raised pattern floor plate for the top flange would permit a decrease in the required number of connectors. It can be seen in Table 2 that only Beam 11 had the number of connectors required by the AISC Specification[2] and that the number decreased in the following order: 11, 12, 14 and 15. Beam 13 had the same number of connectors as Beam 14 but it had a different shape of the steel section (Fig. 2).

Deflections and slips for all beams of this group are shown in Figs. 9 and 10 as functions of the ratio of applied moment M to the theoretical ultimate moment M_u. Table 3 gives the observed ultimate moment M_m and slip at failure. The same table also gives the theoretical values for the yield moment M_y, and the theoretical ultimate moments for composite beam with adequate shear connection M_u, for composite beam with inadequate shear connection M_u', and for non-composite beam M_{ps}. In Table 4 comparisons are made between observed and theoretical ultimate moments.

Beams 11 and 12 failed in flexure after considerable deformation, indicating good plastic action. Beams 13, 14a, 14b and 15 failed in shear after relatively small amounts of plastic deformation and failed to develop the theoretical ultimate moment M_u. Comparisons in Figs. 9 and 10 show that the ultimate load and the deflection at ultimate load decreased with decreasing number of connectors, and the end slip at ultimate load increased rapidly as the number of shear connectors was decreased.

It is apparent from the ratios M_m/M_u in Table 4 that, as far as the ultimate strength is concerned, the floor plate did not replace effectively the connectors omitted from specimens 12 through 15. The questions then remain whether the floor plate contributed at all to the ultimate strength of the beams and whether it altered the behavior at working loads.

The ultimate moment M_u was computed on the assumption, shown in Fig. 11b, that the connection is adequate. For beams with fewer than the adequate number

Table 3. Summary of Beam Test Results

Specimen Number	Type of Failure	M_m ft-kips	Theoretical Values				End slip at failure, in.
			M_u ft-kips	M_u' ft-kips	M_y ft-kips	M_{ps} ft-kips	
11	Flexure	217.7	194.5	—	142.5	83.2	0.0787
12	Flexure	207.3	198.7	188.0	142.5	90.9	0.0900
13	Shear	169.6	182.5	140.0	119.5	95.4	0.1332
14a	Shear	161.5	203.0	154.0	142.5	90.9	0.1582
14b	Shear	172.2	198.2	153.0	142.5	90.9	0.1305
15	Shear	139.1	198.0	130.5	142.5	90.9	0.1954
21	Flexure	177.7	159.6	—	119.5	86.7	0.0400
22a	Flexure	364.6	334.0	—	133.3	113.4	0.1504
22b	Flexure	364.6	342.0	—	133.3	113.4	0.1320
23	Flexure	244.3	212.0	—	133.3	104.4	0.0305
32	Shear	395.8	369.0	—	173.5	118.4	0.1710
33a	Flexure	361.3	331.0	—	184.5	123.9	0.0271
33b	Flexure	367.8	334.0	—	184.5	123.9	0.0200
34	Flexure	253.1	214.1	—	137.1	115.2	0.0650
35	Flexure	521.1	487.5	—	314.0	177.5	0.0492
41a	[a]	251.5	229.0	—	170.6	73.7	0.0115
41b	Flexure	234.6	215.0	—	170.6	73.7	0.0048

[a] *Concrete shear failure*

of connectors attached to a smooth top flange, the ultimate strength of the beam is governed by the aggregate strength of the connectors.[9] The stress distribution for such a beam with inadequate connectors is shown in Fig. 11c. Assuming that the ultimate strength of the individual studs was 12.1 kips,[9] the corresponding moment M_u' was computed for Beams 12 through 15 and compared with the test moment in the last column of Table 4.

The test moment M_m exceeded the computed moment M_u' in every case. However, except in Beam 13, the ratio M_m/M_u' was of the same order of magnitude as the ratio M_m/M_u for Beam 11. Thus, no contribution of the floor plate to the strength of Beams 12, 14 and 15 has been demonstrated. On the other hand, Beam 13 was stronger than indicated by the theoretical moment M_u', suggesting that the wider floor plate of this specimen was effective in increasing the strength of the beam.

The effect of the floor plate on deformations at working load level may be estimated qualitatively from Figs. 9 and 10. It can be seen that while the end slips in Beams 12 through 15 exceeded those measured in Beam 11 even at loads of the order of $M/M_u = 0.4$, these increased slips did not result in increased deflections. For example, at the moment level of 0.5 M_u, which has been suggested as the working moment,[9] the deflection of all specimens was about 0.3 in. Because of the small number of connectors in specimens 13 through 15, these results suggest strongly that the floor plate effectively increased the degree of interaction at working load level.

Table 4. Comparison of Test Results with M_u and M_u'

Specimen Number	Type of Failure	M_m/M_u	M_m/M_u'
11	Flexure	1.118	—
12	Flexure	1.041	1.102
13	Shear	0.928	1.210
14a	Shear	0.795	1.050
14b	Shear	0.868	1.125
15	Shear	0.702	1.065
21	Flexure	1.112	—
22a	Flexure	1.110	—
22b	Flexure	1.065	—
23	Flexure	1.152	—
32	Shear	1.072	—
33a	Flexure	1.092	—
33b	Flexure	1.103	—
34	Flexure	1.180	—
35	Flexure	1.070	—
41a	[a]	1.098	—
41b	Flexure	1.092	—

[a] *Concrete shear failure.*

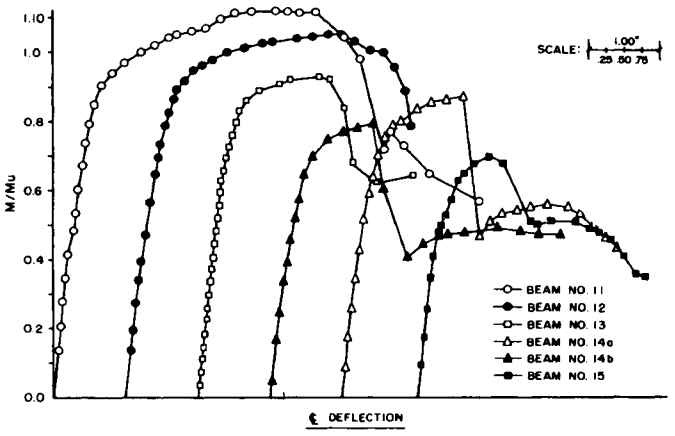

Fig. 9. Plot of M/M_u vs. centerline deflection for Series 1 beams

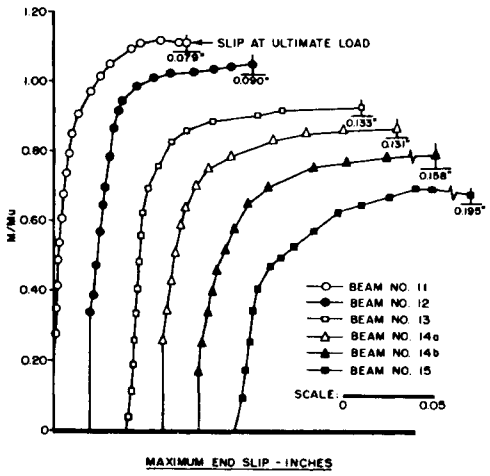

Fig. 10. Plot of M/M_u vs. maximum end slip for Series 1

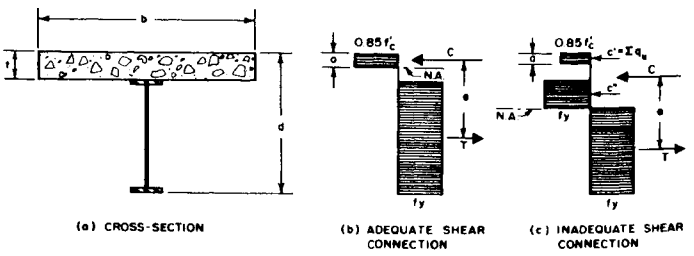

Fig. 11. Stress distribution at ultimate moment for beams with steel section of one yield strength

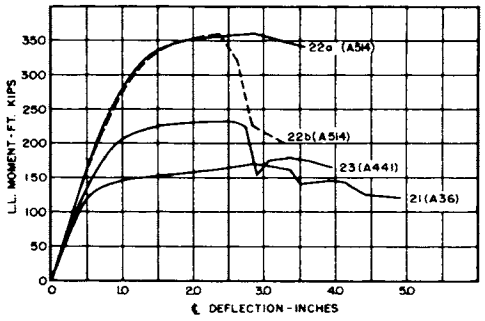

Fig. 12. Series 2, experimental moment-deflection curves

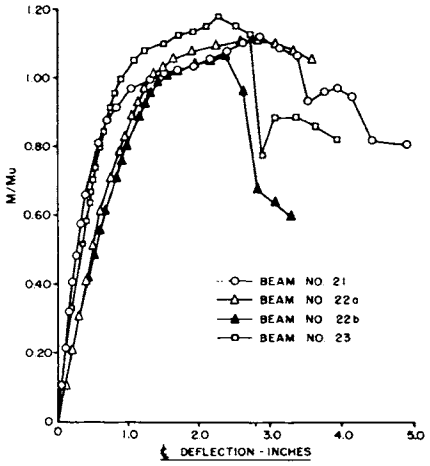

Fig. 13. Plot of M/M_u vs. centerline deflection for Series 2

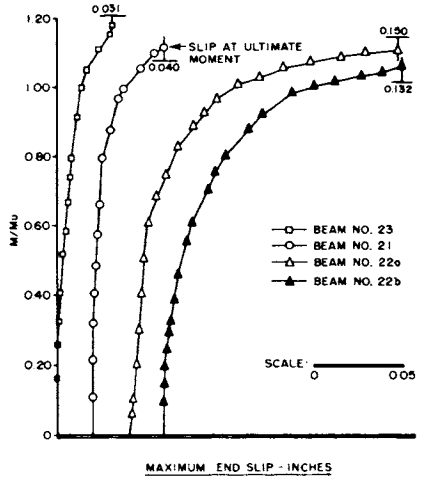

Fig. 14. Plot of M/M_u vs. maximum end slip for Series 2

Series 2—The objective of this series was to study the structural behavior of composite beams with hybrid steel sections. The top flange and the web in all beams was of A36 steel, but the bottom flange was of A36, A441 or A514.

The experimental moment-deflection curves for the four beams are shown in Fig. 12. It is apparent that the ultimate strength increased and the deflection at ultimate load tended to decrease with increasing strength of the bottom flange.

All four beams failed in flexure and developed the theoretical ultimate moment (Table 3). The ratio of the test to theoretical ultimate moment M_m/M_u was always in excess of 1.0 (Table 4), but the excess was the lowest for Beams 22a and 22b having only 72 percent of connectors required by the AISC Specification[2], and the largest for Beam 23 having 138 percent of the required minimum number.

It is noteworthy that the stiffness at working load levels (Fig. 12) was about the same for all beams. The absolute deflection at working load level was, of course, higher in the stronger beams (Fig. 13). But the load deflection curves were essentially straight even at moments in excess of 0.5 M_u. Thus the connectors were adequate both from the standpoint of strength and the standpoint of beam stiffness.

The magnitude of end slip at failure in Beams 22a and 22b (Fig. 14) indicated that the failure of the connectors in these beams was imminent.

Series 3 The objective of this series was to study the structural behavior of composite beams with hybrid steel sections having high strength steel not only in the bottom flange but also in the lower part of the web, and to compare the behavior of such beams with the corresponding beams of Series 2. In Beam 32, the bottom flange was of A514 steel and the lower part of the web was of A441 steel. In Beams 33a and 33b, the bottom flange was of A441 steel and the lower part of the web was of A514 steel. In Beams 34 and 35 the bottom flange and the lower part of the web were of identical steel: A441 in Beam 34 and A514 in Beam 35, as shown in Fig. 2.

All five beams developed the theoretical ultimate moment M_u of the composite section (Table 3) and, except for Beam 32, failed in flexure. Beam 32, having 74 percent of the connectors required by the AISC Specification, failed in shear at an end slip of 0.171 in. (Fig. 15) at a load exceeding the theoretical ultimate moment.

The balanced failure of Beam 32 permits calculation of the ultimate strength of the $^1/_2$-in. studs. At flexural

failure, the steel section had yielded through the full depth. Thus the horizontal force acting on the connectors in one shear span is equal to the area of the steel section times the yield point. In Beam 32 the average shear load per connector at failure was 14.6 kips. In Beams 22a and 22b, for which the magnitude of slips indicated that failure of connectors was imminent, the average loads per connector computed as outlined above were 14.6 and 14.4 kips, respectively.

The flexural failures of Beams 33a, 33b and 35 occurred suddenly and with little warning (Fig. 16). The sudden failure was probably caused by the fact that a relatively large depth of the slab was subjected to high compressive stresses.

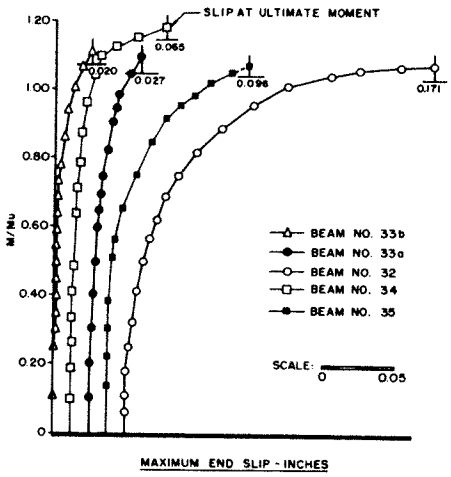

Fig. 15. Plot of M/M_u vs. maximum end slip for Series 3

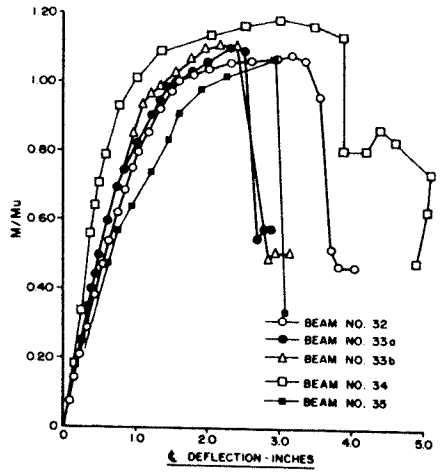

Fig. 16. Plot of M/M_u vs. centerline deflection for Series 3

The effect of the presence of high strength steel in the web is illustrated by the moment-deflection curves in Fig. 17. In this figure the type of steel used in the lower web is given in parenthesis. It is apparent that while the comparable beams of Series 2 had lower ultimate strength because of the weaker web, their stiffness in the range of working loads was essentially the same as the stiffness of Series 3 beams. The slight increase in stiffness in the elastic range for Beam 35 is due to dimensional differences. The plate thicknesses for this beam were larger than the thicknesses of the other beams. Further, the relatively larger capacity for Beam 35 is due to the unusually high yield strength of the A514 steel plate in the web.

Particularly interesting is a comparison between Beams 23 and 34. The A441 steel in the web of Beam 34 extended far enough so that the current AISC Specification[2] would permit the full design stress of 33 ksi to be used in the bottom flange of this beam. The absence of the A441 steel in the web of Beam 23 would require that the design stress for the flange of this beam be reduced to 24 ksi, a decrease of 28.2 percent. Yet the ultimate test moment of Beam 23 was only 3.5 percent less than that of Beam 34, and the deflections of the two beams were practically identical in the working load range.

Series 4—The objective of this series was to observe the behavior of a composite beam with the steel section in the shape of an inverted T. The two specimens of this series were of the same design.

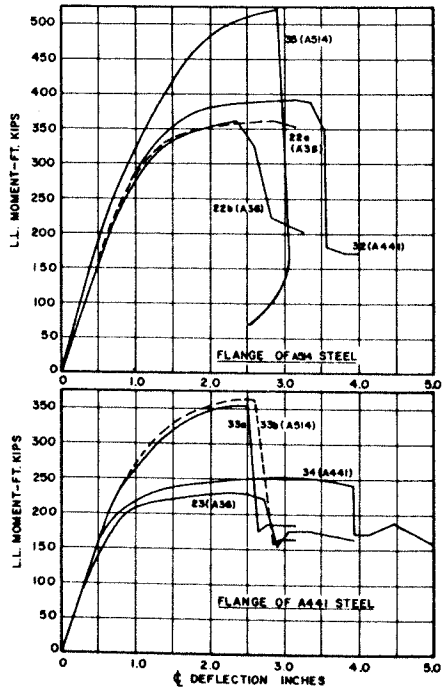

Fig. 17. Comparisons between Series 2 and 3 beams

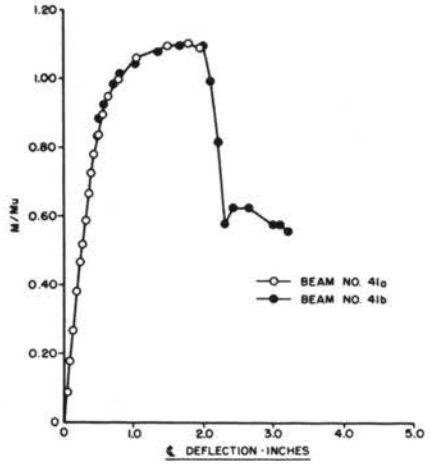

Fig. 18. Plot of M/M_u vs. centerline deflection for Series 4

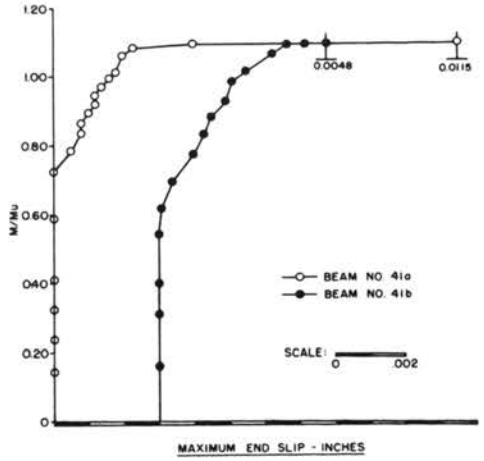

Fig. 19. Plot of M/M_u vs. maximum end slip for Series 4

The deflections and slips, plotted in Figs. 18 and 19 as functions of M/M_u, show that the two specimens responded to loading in essentially the same manner until the ultimate load was reached. There was no slip and the load deflection curve was linear beyond the working load level. After the first end slip occurred, the slip continued to increase in both specimens at about the same rate until the moment slip curve leveled off at ultimate load. From then on the two beams responded differently.

In Beam 41a the slip continued to increase without appreciable change in the load and herringbone cracking developed on the top surface of the slab (Fig. 20), indicating failure by shear in the concrete. The test was stopped when the beam refused to carry additional load, soon after the maximum moment was reached.

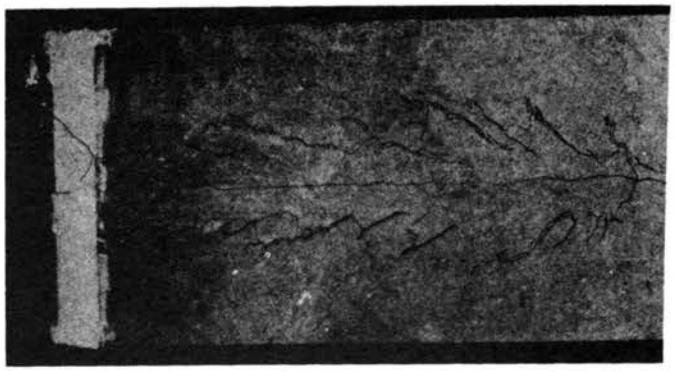

Fig. 20. Top view of slab in Beam 41a, showing the herringbone cracking in the concrete. Such cracking did not prevent the beam from surpassing its calculated capacity.

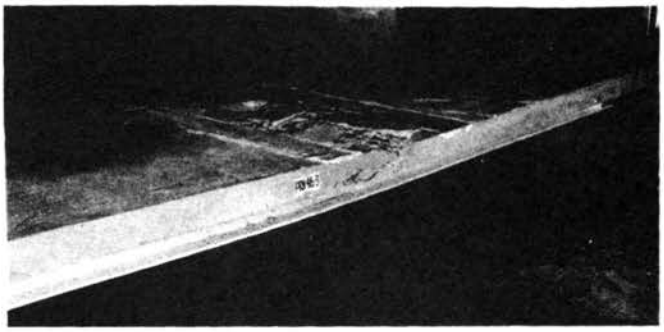

Fig. 21. View of Beam 41b. Note the absence of herringbone type cracking in this beam. Collapse was due to flexural failure (crushing of concrete slab).

Beam 41b failed in flexure at a very small end slip. Figure 21 shows the crushing of the slab in this beam. The post-failure behavior of Beam 41b was remarkably good. The steel section and the remainder of the slab were able to maintain a load considerably in excess of the capacity of the steel section alone.

The difference in the failure of the two specimens would suggest that the design represented a balance between a flexural failure and a failure by shear in the slab. However, some evidence suggests that the mode of failure of Beam 41a may have been caused by faulty testing techniques.

Both beams failed at moments in excess of the theoretical ultimate moment M_u (Table 3).

The data for Beams 41a, 41b, 11 and 21 illustrate the well known fact that the unsymmetrical steel section is particularly efficient for composite beams. The four beams had the same steel area and were made of the same steel. The moment deflection curves, shown in Fig. 22, show clearly that the symmetrical section was the least efficient while the inverted T section was the most efficient. Series 4 beams were 44 percent stronger than Beam 21 with the symmetrical steel section.

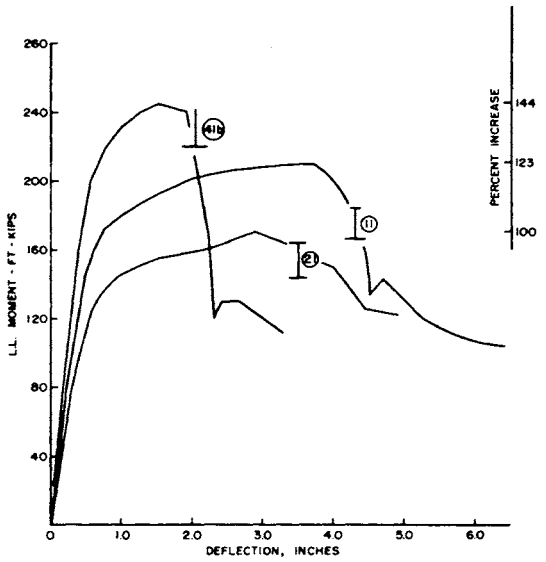

Fig. 22. Comparison of symmetrical and unsymmetrical sections of A36 steel

CONCLUSIONS

Based on the results of this investigation, which was of an exploratory nature, the following conclusions are tentatively drawn:

1. The use of the hybrid steel sections in composite beams was shown to be feasible. The hybrid beams developed the calculated full plastic strength M_u. However, their rotation capacity (toughness) was somewhat smaller than that of the composite beams with A36 steel sections.
2. Except for increased strength, there was no significant benefit derived from the high strength webs in the hybrid composite beams.
3. Steel sections without top flanges made very efficient composite beams. Because only two tests were made and differences were observed in the mode of failure of the two beams, further studies of this type of beam are desirable.
4. The floor plate appeared to be effective in reducing end slip and deflection at working load level. However, except in a specimen with a wider plate, it did not increase materially the ultimate strength of these beams with inadequate shear connection.
5. The AISC provisions for the design of stud shear connectors provided adequate factor of safety against shear failure and insured relatively small slips.
6. The ultimate strength of a ½-in. diameter stud in the composite beams was approximately 14.6 kips.

ACKNOWLEDGMENTS

This investigation was carried out under a research grant from the Committee of Steel Plate Producers of American Iron and Steel Institute and under the supervision of the Joint Engineering Subcommittee of the Committee of Steel Plate Producers and the Committee of Structural Steel Producers. Most of the work reported herein was carried out under the direction of the writer by Mr. J. W. Hall, Jr. The writer expresses his appreciation to Mr. Hall for his excellent performance, initiative and assistance.

The author takes this opportunity to thank Dr. Ivan M. Viest for the technical guidance he provided in his capacity as project supervisor for the Joint Engineering Subcommittee and for his continued interest in this project.

The investigation was carried out in the Materials Laboratory of the Department of Civil Engineering at the University of Texas. Appreciation is expressed to the staff of the laboratory and to the many graduate and undergraduate students who assisted in this project. Thanks are also due for the splendid cooperation and help given by the staff of the Bureau of Engineering Research, College of Engineering.

REFERENCES

1. *American Association of State Highway Officials* Standard Specifications for Highway Bridges *7th Edition, Div. I, Sect. 9, 1957.*
2. *American Institute of Steel Construction* Specification for the Design, Fabrication, and Erection of Structural Steel for Buildings *New York, N. Y., 1963.*
3. *Joint ASCE-ACI Committee on Composite Construction* Tentative Recommendations for the Design and Construction of Composite Beams and Girders for Buildings *Proceedings ASCE, Structural Division, December, 1960, pp. 73–92.*
4. *Culver, C., Zarzeczny, P. J. and Driscoll, G. C.* Composite Design for Buildings *Progress Report No. 1, Fritz Engineering Laboratory Report No. 279.2, Lehigh University, June, 1960.*
5. *Culver, C., Zarzeczny, P. J. and Driscoll, G. C.* Composite Design for Buildings *Progress Report No. 2, Fritz Engineering Laboratory Report No. 279.6, Lehigh University, January, 1961.*
6. *Viest, I. M., Fountain, R. S. and Singleton, R. C.* Composite Construction in Steel and Concrete *McGraw-Hill Book Company, New York, N. Y. 1958.*
7. *Toprac, A. A. and Engler, R. A.* Plate Girders with High-Strength Steel Flanges and Carbon Steel Webs, *Proceedings, 1961 National Engineering Conference, American Institute of Steel Construction, New York, N. Y., pp. 83–94.*
8. *Toprac, A. A. and Hall, J. W.* Strength of Three New Types of Composite Beams *SFRL Report No. 01, Department of Civil Engineering, The University of Texas, December, 1964.*
9. *Slutter, R. G. and Driscoll, G. C.* Composite Design for Buildings *Progress Report No. 3, Fritz Engineering Laboratory Report No. 279.10, Lehigh University, January, 1962.*

STRENGTH OF THREE NEW TYPES OF COMPOSITE BEAMS

(Test Procedure)

PART II

DESCRIPTION OF TEST SERIES AND SPECIMENS

The investigation was divided into four series with seventeen specimens as outlined in Table 1. For every specimen the span and the concrete flange were identical. All specimens had the same depth of steel section below the slab, the same area of steel, and the same web thickness. This gave a basis for direct comparisons of the test results. It also allowed a great deal of latitude in the design of each separate series to best suit its own individual objective.

The design of all specimens was based on ultimate strength principles. Figure (11b) in Part I shows the internal couple and the rectangular stress block profile. It is generally accepted that the ultimate strength of composite sections can be predicted accurately by these principles. However, adequate interaction between the concrete flange and the steel section must be provided; and the properties of the materials involved must be known.[3, 4, 5] The assumed ultimate design strengths were: $f_c' = 3000$ psi, f_y of A36 $= 36$ ksi, f_y of A441 $= 50$ ksi, and f_y of A514 $= 100$ ksi; where f_y equals the static yield point of steel and f_c' equals the cylinder strength of concrete at the age of testing.

It was desired that all steel sections of each series be the same in depth, have the same area of steel, and have the same thickness of flanges and webs. This is illustrated in Table 1 and Figure 2 (see Part I). For reasons of uniformity of the experiment, it was important that all webs and flanges be cut from the same plate. The choice of steel sections was arrived at by a procedure in which the primary considerations were:

(a) that the web be adequate to resist the applied shear at a relatively low value of average shear stress at working levels.

(b) that the neutral axis of the composite section be located outside the steel section when the ultimate moment was attained.

The design of all shear connectors was based on the procedure outlined in Section 1.11 of the AISC Specification for the Design, Fabrication and Erection of Structural Steel for Building, assuming a concrete strength of 3000 psi.

The concrete flange of all specimens represented a typical floor slab of a building; and each concrete flange had the same dimensions. Physical limitations of the testing machine dictated that the concrete flange width not exceed 47″. In order that the full width of compression flange be effective, a thickness of 4″ was chosen for the top concrete flange. For composite construction, 4″ is close to the minimum practical thickness for the concrete structural slab. An eight foot beam spacing was chosen for the design of the slab steel reinforcement, although normal composite construction tends toward maximum spacing of beams. Reinforcement was proportioned to leads which are typical of modern office building loading, i.e., 60 psf live load, 20 psf partition and 10 psf ceiling. The bars used were #3 at 8″ o. c. for top steel and at 10″ o. c. for bottom steel resulting in 0.62% of reinforcing. Temperature reinforcing, consisting of a total of seven #2 bars, was placed longitudinally. This is slightly under 0.002 bt required by the American Concrete Institute (ACI) Code.

The following discussion gives a description of the test series from 1 to 4, and the design of each specimen: Figures 1 and 2 and Tables 1 and 2 give pertinent information regarding the specimens. Since shear was nearly constant in all specimens, the shear connectors were uniformly spaced between the reaction point and the nearest load. One pair of connectors was used at midspan in all specimens. Table 2 shows the size, number, spacing and percent of AISC requirements of shear connectors used for each test. From this table, the number of connectors per shear span may be compared to the requirements of the AISC Specification.

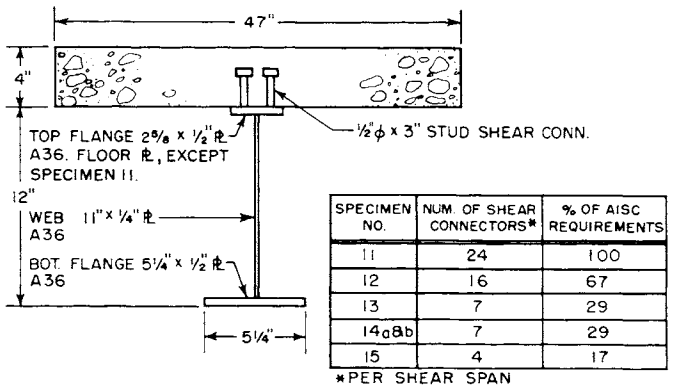

SPECIMEN NO.	NUM. OF SHEAR CONNECTORS*	% OF AISC REQUIREMENTS
11	24	100
12	16	67
13	7	29
14a&b	7	29
15	4	17

*PER SHEAR SPAN

FIGURE 23 DESIGN DETAILS OF SERIES I SPECIMENS

Series 1. In this series, there were six beams, 11, 12, 13, 14a, 14b, and 15 (see Figure 23). Beam 14b was a duplicate of 14a. All specimens, except 13, were made with an unsymmetrical steel section. Specimen 11 was the control beam of the group. This beam had a smooth plate for the top flange and shear connectors based on 100% of the requirements of the AISC Specification. Beam numbers 12, 13, 14 and 15 had a top flange using floor plate (see Appendix A for details), and a decreasing percentage of AISC required shear connectors. Specimen 13 had symmetrical flanges like the steel sections tested in Series 2; consequently, this specimen had a larger number of floor plate deformations than beams 12, 14 and 15.

Figure 23 gives details of this group of specimens. The total area of steel in the composite section including the flanges and web was established. Using ½″ thick plate, it was now necessary to proportion the area between the top and bottom flanges for the unsymmetrical steel shapes.

An unsymmetrical section was desired with minimum area in the top flange; the only restriction being that the width of the flange would accommodate easy installment of two $\frac{1}{2}$" diameter headed studs. The width chosen was 2-$\frac{5}{8}$", leaving for the bottom flange a width of 5-$\frac{1}{4}$". The number of shear connectors used in this series varied from 100 percent to approximately 17 percent of the AISC requirement. All of the shear connectors for this series were in a single row. Beam 15 had the smallest number of shear connectors, four in each shear span. This number of connectors was thought to be the minimum necessary to resist shrinkage stresses and facilitate handling. Specimen 13 was the only symmetrical section in this group of specimens. Its design was based on that for Series 2. This specimen was introduced in Series 1 so that a comparison with 14a and 14b specimens could be made. This was to establish the effect of plate deformations on structural behavior.

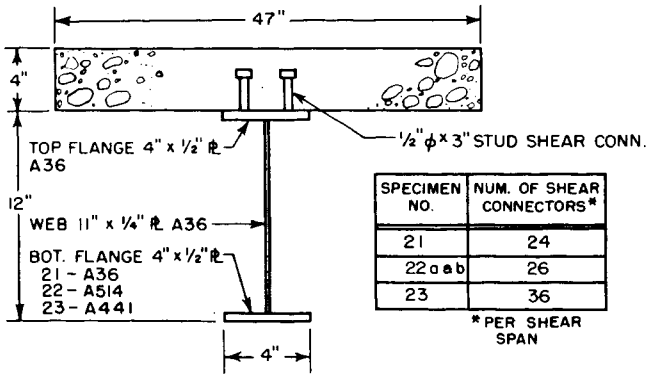

FIGURE 24 DESIGN DETAILS OF SERIES 2 SPECIMENS

Series 2. This series was composed of beams 21, 22a, 22b and 23 (see Figure 24). All specimens were made with symmetrical steel sections; the only variable being the yield strength of the bottom flange. Specimen 21 was the control beam of this group with a cross sectional steel area composed entirely of ASTM A36 plate. Specimens 22 and 23 had bottom flanges of ASTM A514 and the high strength A441 steel, respectively. Specimen 22b was a duplicate of 22a.

Composite construction is covered under Part I of the 1961 AISC Specification in which members are proportioned by allowable working stress provisions based on a percentage of the yield point. At present, the Specification does not allow the design of composite beams under the provisions of Part 2 for plastic design. The use of ASTM A441 steel is allowed in Part 1. However, the combination of an ASTM A36 web and an A441 bottom flange would violate the stress provisions of the Specification if the A441 steel was stressed to its allowable limits. It has been shown that hybrid steel girders perform satisfactorily despite the difference in yield strengths of the web and flange.[7]

The use of A514 steel is not covered by the current AISC Specification. A hybrid girder, such as 22a or b, employing an A36 web, A514 flange with a yield strength of 100,000 psi, would also violate the working stress provisions of Part 1 of the AISC Specification.

The objective of this series was to determine whether the hybrid steel sections perform satisfactorily in composite beams. Figure 24 gives details of the steel section and shear connectors for the specimens used in this series.

Series 3. This series, composed of beam numbers 32, 33a, 33b, 34 and 35 was an extension of Series 2. All beams were symmetrical in cross section. However, the steel sections in this series had portions of their lower webs fabricated of steels with higher yield strength than A36. The primary objective of these tests was to determine if there is any necessity for having part of the web of hybrid composite beam in high strength steel. This is required to conform to current working stress limitations of the AISC Specification.

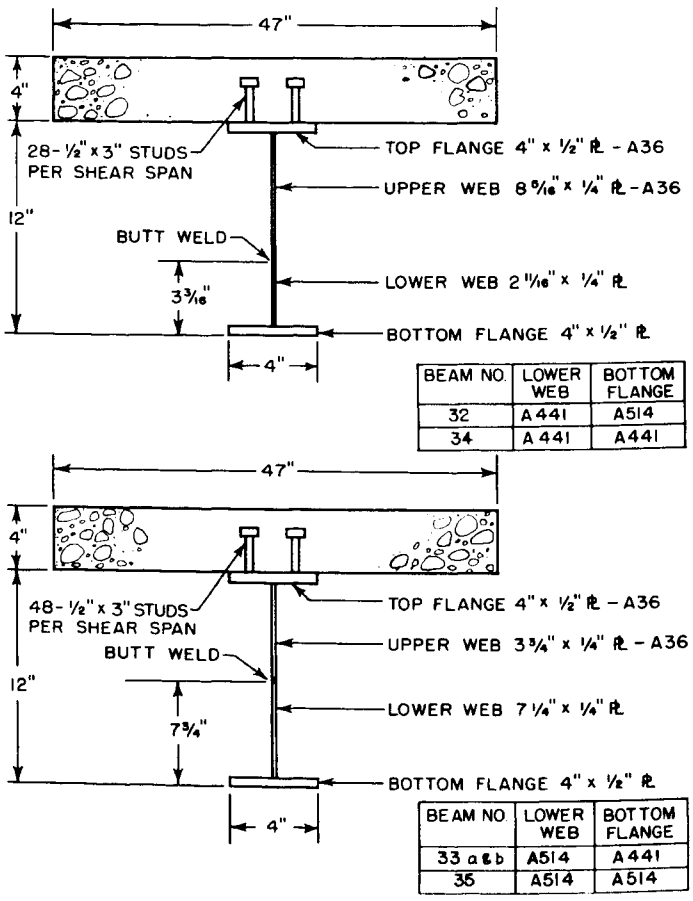

FIGURE 25 DESIGN DETAILS OF SERIES 3 SPECIMENS

The details of these specimens for this series are given in Figure 25. For beams 34 and 35 the lower part of the web and lower flange are the same material, either A441

or A514 steel. The depths of the high strength portion of the web were arrived at by assuming linear stress distribution. The top of the high strength portion of the web was the point at which the bending stress was equal to the allowable stress for A36 steel. Beam 32 had A514 steel for the bottom flange with A441 steel in the lower portion of the web; while beams 33a and 33b had A441 for the bottom flange with A514 steel in the lower portion of the web.

Series 4. It was the purpose of this test to explore the possibility of eliminating altogether the top flange of the steel section of a composite beam by attaching the shear connectors to the web. This type of composite beam section was used in a short span bridge.* However, no research has been reported. Only one beam and a duplicate were tested. Figure 26 shows the details of the beams of this series.

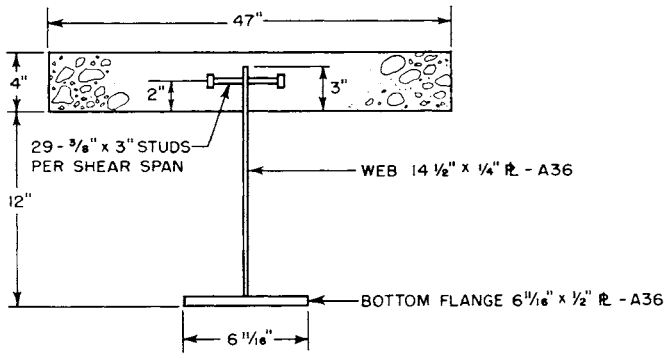

FIGURE 26 DESIGN DETAILS OF SERIES 4 SPECIMENS

The web was extended into the slab for attachment of shear connectors, thereby resulting in slightly more web area than the beams of the other series. The remaining portion of the total steel area, which was constant for all beams, was incorporated in the bottom flange. Three-eighth inch diameter studs were substituted for the ½" diameter studs which were used in the other tests of this program. Because of the relative thinness of the web to which these studs were attached, it was thought that there could be a possibility of tearing the web material before a flexural or shear failure occurred if the larger studs were used.

FABRICATION OF TEST SPECIMENS

The steel sections for all series were fabricated by a commercial fabricating shop from working drawings prepared at The University of Texas. All studs were shop welded by the fabricator from stock on hand. The specimens of Series 1 and 4 were badly warped from fabrication stresses.

The concrete for all specimens was mixed in the laboratory, using local river gravel, sand and high early strength cement. The mix was designed to give a 7-day strength of 3000 psi with a 6" slump. The actual cylinder strengths for the concrete in each specimen are presented with the test results. Quality control consisted of adjusting the amount of water until the desired slump was achieved. If the amount of water required to make the slump 6" was greater than the calculated batch water, based on moisture content of aggregates, slurry was added to maintain the water-cement ratio. Since the maximum permissible batch size was slightly in excess of 11 cubic feet, which was only one half of the volume required to fill the form and test cylinders, two batches were used in all beams. All test specimens were cast in a plywood form designed for easy stripping and multiple reuse.

Before casting the composite flange, all shear connectors on the steel section were inspected for soundness with a hammer. Those connectors which were bent about 30 degrees from the vertical in testing were straightened back. All faulty connectors and those that were cracked during this testing were replaced or rewelded before the steel beam was placed in the form.

After leveling the form, and plumbing the steel web, all joints were taped and the forming surface was given a heavy coat of form oil. Care was taken not to get any oil on the beam or shear connectors. Reinforcing mats were prefabricated for all specimens and placed in the forms on slab bolsters and continuous high chairs. The highest quality concrete, judging from the wet mix, was placed in the center portion of the beam and three standard test cylinders were made. Two cylinders were made from the remaining batch which was placed in the ends of the specimen. The concrete was thoroughly vibrated with an internal vibrator to insure a dense slab free of honeycombing.

The slab was steel troweled to a smooth finish and then covered as soon as possible with a mat for wet curing. The specimen was kept damp for three days after which time it was allowed to dry until testing. As nearly as possible, all test cylinders were subjected to the same curing conditions as their companion beam specimens. Lifting attachments were bolted to the web of the specimens at each end. These attachments were hooked to floor cranes by means of chain slings. Care was taken to prevent the beams from tipping over, or being damaged during their movement from the casting yard to the laboratory and testing machine.

TEST PROCEDURE AND INSTRUMENTATION

Beams were selected for testing in a random manner in

Delameter, R. S., "Experimental Design for Short-Span Bridges," Modern Steel Construction, American Institute of Steel Construction, New York, Vol. III, No. 2, Second Quarter, 1963, pp. 10-12.

an effort to eliminate systematic experimental errors.

The composite beam specimens were moved from the storage area and carefully positioned and aligned in the testing machine. Great care was taken to place the concrete flange level and the steel web plumb. Figure 27 shows the details of a typical beam ready for testing.

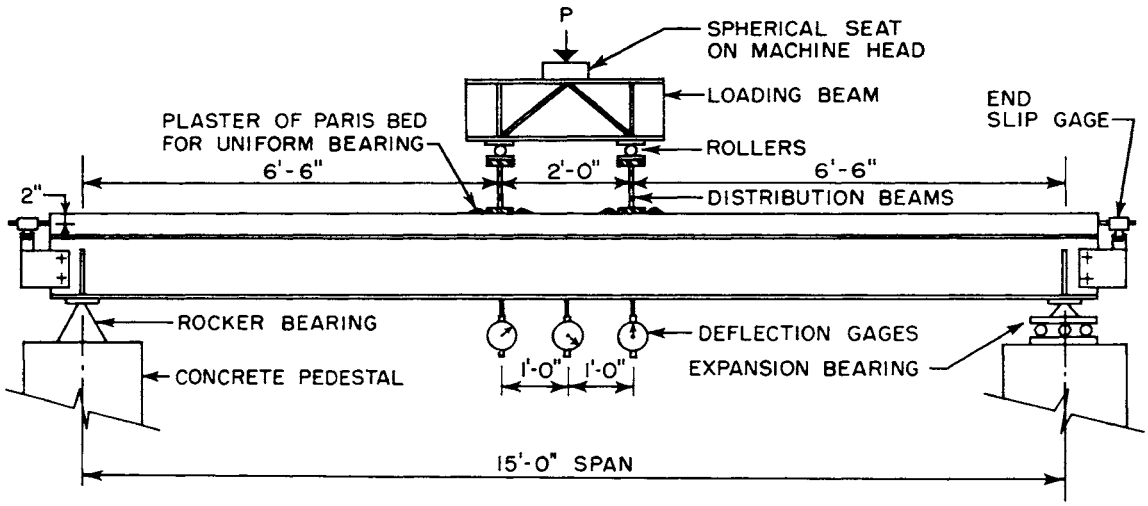

FIGURE 27 DETAILS OF TEST SET-UP

After the beam was properly located in the machine, measurements were made of the concrete flange and steel section. Table 5 shows the average dimensions taken in the constant moment region. The steel beam was then given a thin coat of whitewash before testing in order that the formation of yield lines could be observed.

Table 5. Averaged Dimensions of Test Specimens Taken In Constant Moment Region

Specimen Number	a Inches	b Inches	c Inches	d Inches	e Inches
11	46.6	4.00	12.0	2.63	5.25
12	46.5	3.96	12.0	2.69	5.25
13	46.5	3.94	12.0	4.00	4.00
14a	46.3	4.00	12.0	2.63	5.13
14b	46.5	4.08	12.0	2.69	5.25
15	46.5	4.00	12.0	2.66	5.28
21	46.63	4.00	11.75	4.06	4.00
22a	46.63	4.00	11.89	4.00	4.06
22b	46.5	4.05	11.75	4.00	4.00
23	46.5	4.02	11.88	4.00	4.00
32	46.63	4.01	12.0	4.00	4.00
33a	46.6	3.94	11.88	4.00	4.00
33b	46.5	3.91	12.05	4.00	4.00
41a	47.25	4.05	12.0	—	6.69
41b	46.44	4.00	12.0	—	6.72

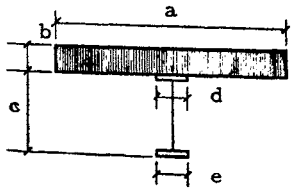

Instrumentation for all beams consisted of two dial gages at the ends to measure slip, and three dial gages symmetrically placed about the centerline of the span to measure deflection and rotation as shown in Figure 27. In addition, beams 32 and 33b were instrumented with electric strain gages, as shown in Figures 28 and 29, in order to study the strain distributions in the shear span and in the constant moment section. The gage length of the electric strain gages was one inch and six inches respectively for the steel and concrete.

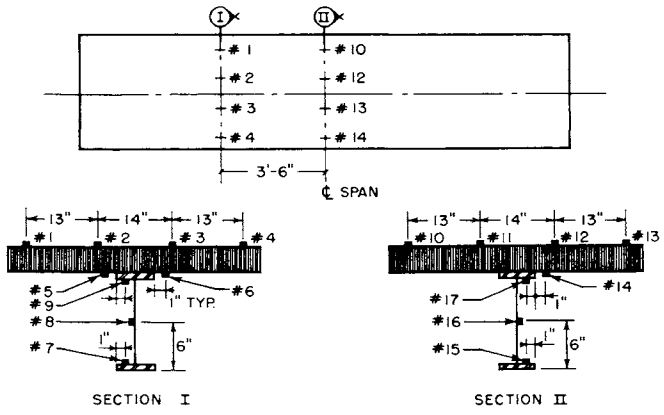

FIGURE 28 LOCATION OF STRAIN GAGES ON SPECIMEN 32

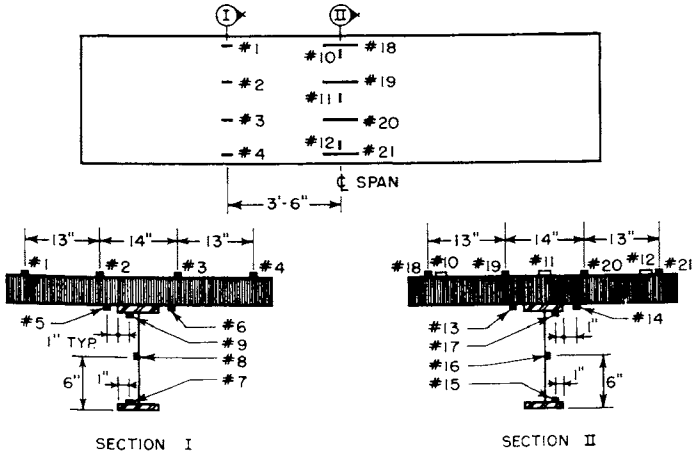

FIGURE 29 LOCATION OF STRAIN GAGES ON SPECIMEN 33a

All specimens were tested in a hydraulic universal testing machine of 200,000 pounds maximum capacity.

Increments of load were chosen that would give at least ten readings between zero and the calculated yield load, P_y. After P_y was exceeded the specimens were loaded so that resulting deflections were about 0.2 inches for each load increment. Due to the effect of yielding and relaxation, the resistance exhibited by the specimen decreased with time. Therefore, after yielding began, the specimen was allowed to creep and relax. Load readings were taken after the rate of drop in the load reached approximately 100 pounds per minute.

TEST DATA AND DETAILS OF RESULTS

In this section, the measured properties of materials (steel and concrete) will be given and discussed. Also further analysis of the beam test results will be presented.

Moment-deflection curves for all specimens are given in Appendix C; and the notes taken during the test of all specimens are tabulated in Appendix D.

Properties of Materials

Steel — ASTM A36 steel, used in all webs and all flanges, was of the same specification and cut from the same plate. The fabricator furnished 18" x 18" pieces of plates used in the fabrication of the various flanges and webs.

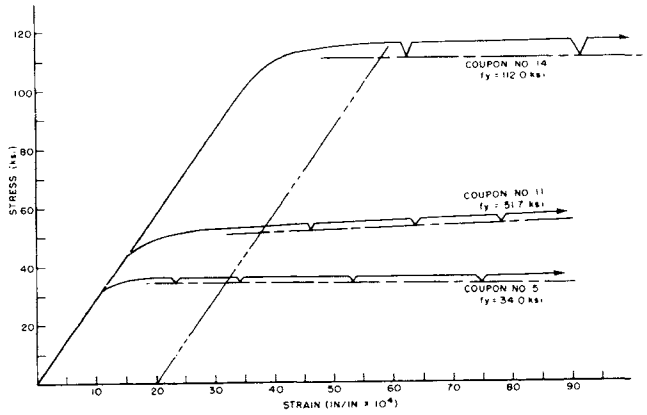

FIGURE 30 TYPICAL STRESS-STRAIN CURVES OF STEELS USED IN PROGRAM

Tensile specimens were made from samples of the plate material used in the steel sections. These specimens were tested to determine the actual yield strengths of the flanges and webs. Figure 30 shows typical stress-strain curves from each type of steel used. Table 6 gives the results of the coupon tests for top flanges, webs and bottom flanges.

Table 6. Mechanical Properties of Steel

Coupon No.	Specification	Specimens to which Values Apply	Location In Beam	Direction of Rolling	Thickness Inches	Yield Point* (ksi)	Average Yield Point (ksi)	Ult. Str. (ksi)
1	A36	11, 21, 22, 23, 32, 33	Top flange	Perpend.	½	36.7		
2	do	do	do	Parallel	½	34.0	34.0**	59.4
3	A36	11, 12, 13, 14, 15, 21, 41	Bottom Flange	Parallel	½	33.2		
4	do	do	do	do	½	33.6	33.4	
5	A36	11, 12, 13, 14, 15, 21	Web	Perpend.	¼	33.7		
6	do	do	do	Parallel	¼	35.8		
7	do	do	do	do	¼	34.4	35.1	
8	A441	23 and 33	Bottom Flange	Parallel	½	56.3		82.8
9	do	do	do	do	½	53.5		80.0
10	do	do	do	do	½	56.2		
11	do	do	do	do	½	51.7	54.4	
12	A441	32	Lower web	Parallel	¼	50.4	50.4	71.0
13	C.A.	32	Lower Flange	Parallel	½	115.2		127
14	do	32	do	do	½	113.2		
15	do	22a	do	do	½	106.0	111.4	
16	C.A.	33a	Lower web	Parallel	¼	105.8		114
17	do	33b	do	do	¼	106.2	106.0	
18	Floor Plate	12, 13, 14, 15	Top flange	Perpend.	½	34.7		
19	do	do	do	Parallel	½	42.7	42.7	
20	Studs	Series 1, 2, 3	—	—	½Φ	—	—	75.4
21	do	Series 4	—	—	⅜Φ	—	—	87.4

* *Refers to static yield point.*

** *Values for perpendicular to rolling direction are not included in the averages.*

Two coupons were prepared from the studs used in this investigation. One coupon was taken from the ½" and the ⅜" diameter stud respectively. The results of these coupon tests are also given in Table 6. These results check quite well with those indicated by the stud manufacturer whose report is given in Appendix B.

Table 7. Results of Concrete Cylinder Tests

Beam Number	Average Compressive Strength — f_c'		Minimum	Maximum
	A psi	B psi		
11	3365	4190	3310	4520
12	3413	3700	3110	3960
13	3930	3585	3570	4060
14a	4456	3600	3600	4330
14b	3283	3550	3250	3580
15	3060	3315	3040	3320
21	3190	4060	3060	4170
22a	2950	—	2700	3090
22b	4356	4370	4180	4460
23	4010	—	3820	4170
32	3580	3840	3500	4110
33a	4800	4570	4360	4930
33b	4830	4645	4650	5030
41a	4770	—	4570	4970
41b	3640	3370	3310	3710

Concrete — Table 7 gives the average compressive strength of the concrete at the time each beam was tested. The average compressive strength, f_c', for the concrete slab area, indicated as "A", was used in the calculation of ultimate moments and elastic deflections. The same table indicates the maximum and minimum strength obtained from all the cylinders for each beam. Note, the smallest minimum value is 2700 psi while the largest maximum value is 5030 psi. However, within each area (A or B) for a given beam, the variation from the average cylinder strength was less than ± 5 percent with one exception.

Definition of Adequate and Inadequate Shear Connection

For further discussion of the beam test results, the shear connection shall be classified as adequate or inadequate according to the following definition based on the equilibrium of horizontal forces acting on the concrete slab at ultimate moment:*

$$\text{Adequate:} \quad \Sigma\, q_u \geq C \geq 1.0$$

$$\text{Inadequate:} \quad \Sigma\, q_u \, C < 1.0$$

where $\Sigma\, q_u$ = the sum of the ultimate shear strength of all the connectors in a shear span, and

C = value of maximum compressive force in the concrete that would develop in the beam when full composite action takes place.

**Slutter, R. G., Driscoll, G. C., "The Flexural Strength of Steel and Concrete Composite Beams," Fritz Engineering Laboratory Report No. 279.15, Lehigh University, March, 1963.*

The measure of the adequacy of the shear connection by the ratios $\Sigma q_u/C$, for all beams based on $q_u = 12.1^k$[9] has been tabulated in Table 4 (Part I). For those beams which had the number of shear connectors recommended by AISC, the ratio $\Sigma q_u/C$ was equal to approximately 1.25. Assuming $q_u = 12.1^k$ for ½" studs and 6.8 for ⅜" studs, all beams with $\Sigma q_u/C > 0.82$ exceeded the theoretical ultimate moment, M_u. The ultimate moment was calculated by the couple illustrated in Figure 11b (Part I). Beams 12, 13, 14a, 14b and 15 were deliberately fabricated with inadequate shear connections. Figure 11c (Part I) shows the cross section profile and the couple used to calculate their ultimate moment M_u'.

Further Study of the Effect of Floor Plate

It was impossible to separate quantitatively the effect of the floor plate from that of the headed studs in the foregoing beams; therefore, the modified ultimate moment, M_u' has been calculated considering only the ultimate shear strength of the studs. M_u', based on a shear value q_u of 12.1 kips, is shown in Table 3 (Part I) for the appropriate beams of Series 1.

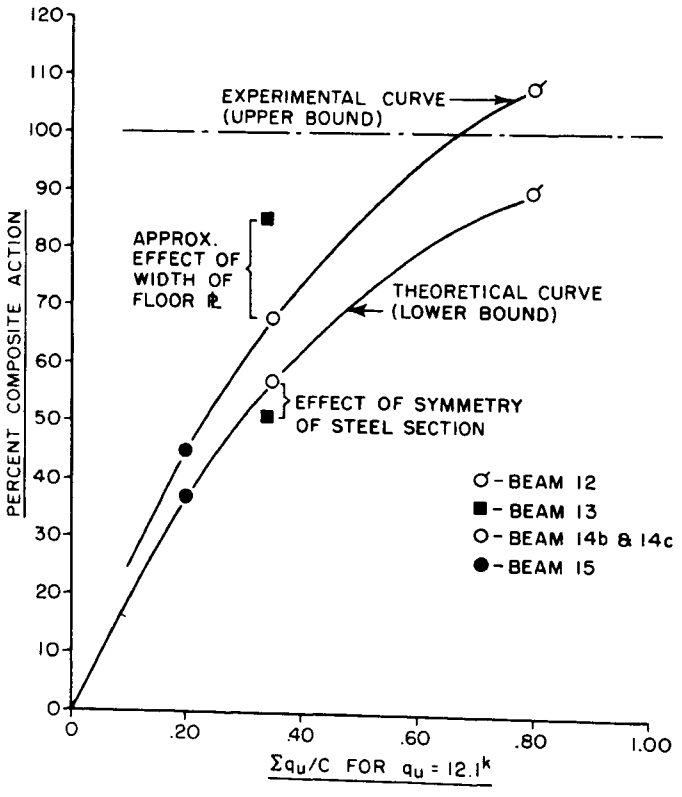

FIGURE 31 PLOT OF PERCENT COMPOSITE ACTION VS. $\Sigma q_u/C$ FOR SERIES I BEAMS WITH FLOOR ℄

Figure 31 is a summary of the results for Series 1 and indicates the quantitative effect of the floor plate on the degree of composite action. Two sets of data are plotted against $\Sigma q_u/C$. For those located on or above the "experimental curve" the ordinate "percent composite action" was computed as

$$\frac{M_m - M_{ps}}{M_u - M_{ps}} \times 100\%$$

and for those located on or below the "theoretical curve" the ordinate was computed as

$$\frac{M_u' - M_{ps}}{M_u - M_{ps}} \times 100\%$$

The difference between the experimental and theoretical values may have been caused either by inaccuracies of the theory or by a beneficial effect of the deformation of the floor plate.

A comparison of the M_m/M_u' — values for beams 12, 14a, 14b, and 15 with M_m/M_u — values for beam 11 and for all beams of Series 2 and 3 (Table 4) suggests that the beneficial effect of the floor plate deformations was very small, if any at all. On the other hand, the data in Table 4 (Part I), as well as in Figure 31, show that in beam 13 with the wider top flange there runs a definite increase in the degree of composite action. The deformations of the floor plate had a substantial beneficial effect in this specimen.

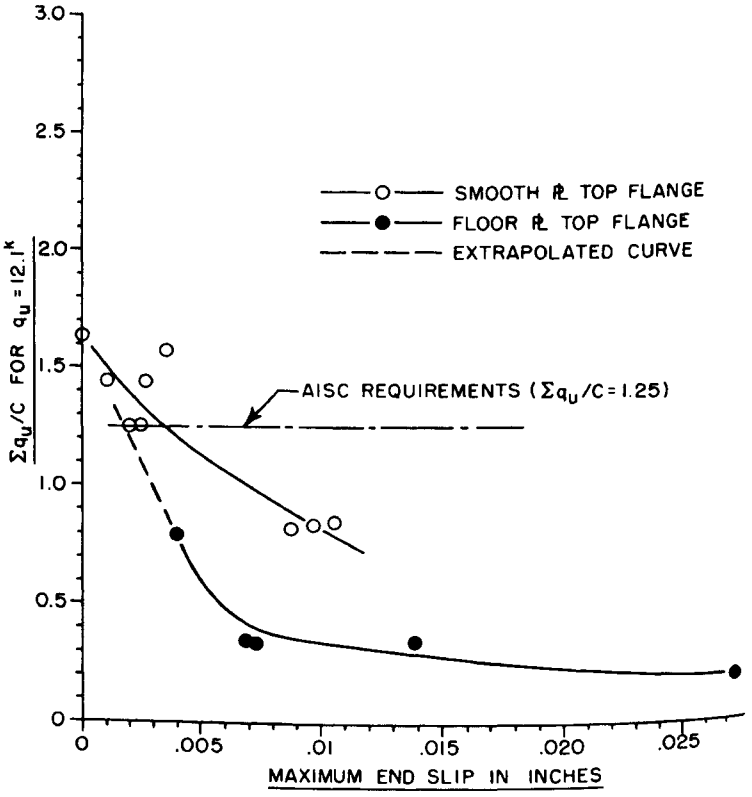

FIGURE 32 PLOT OF $\Sigma q_u/C$ VS. MAXIMUM END SLIP AT 0.5 M_u

Figure 32 shows a plot of $\Sigma q_u/C$ versus maximum end slip for all beams tested. Two curves have been drawn, one representing the beams having a smooth plate for the top flange, and the second representing those beams with the

floor plate for the top flanges. The lower curve, which represents the specimens with floor plate for the top flanges, was extrapolated at its upper end by assuming that both curves would pass through the same point at zero end slip. Figure 32 shows there was no data for a floor beam with floor plate at or near $\Sigma q_u/C = 1.5$. Figure 32 illustrates that the floor plate as a top flange can be very effective in reducing the end slip at working loads. At $\Sigma q_u/C = 1.25$, the specimens with the floor plate showed about 50 percent less slip than those with the smooth plate. As $\Sigma q_u/C$ decreased, the effect of the floor plate became more pronounced. For a given number of shear connectors, and a given $\Sigma q_u/C$, the end slip was reduced by the use of the floor plate.

Further Comparisons of Beam Behavior

Beam performance data at 0.5 M_u are summarized in Table B. A measure of the elastic behavior is defined by the ratio $\frac{\Delta_T}{\Delta_E}$ where Δ_T is the measured centerline deflection; and Δ_E is the calculate theoretical elastic deflection at 0.5 M_u. This ratio varied more in Series 1 than in any other group as expected. It should be noted that beam 13 which had wider flanges than 14a or 14b had the best elastic performance in Series 1. The end slips for all beams shown in Table B of this series also indicate that the floor plate is effective in providing uniform shear connection for elastic action. Except for beam 15, the end slips for Series 1 at working levels were comparable to those of Series 2 and 3.

Table 8. Comparison of Beam Performances at 0.5 M_u

Beam Number	$\frac{\Delta_T}{\Delta_E}$	$\frac{\Delta_T}{L/360}$	End Slip (Inches)	$M_m/0.5\,M_u$
11	1.225	0.542	.0027	2.240
12	1.330	0.602	.0040	2.085
13	1.144	0.542	.0073	1.856
14a	1.450	0.670	.0138	1.590
14b	1.348	0.609	.0069	1.736
15	1.700	0.767	.0275	1.404
21	1.410	0.578	.0020	2.224
22a	1.163	1.010	.0090	2.220
22b	1.190	0.904	.0106	2.130
23	1.250	0.690	.0035	2.304
32	1.184	1.152	.0097	2.142
33a	1.132	0.990	.0027	2.184
33b	1.126	0.993	.0010	2.206
41a	1.172	0.504	.000	2.196
41b	1.235	0.496	.000	2.184

Beam 21 shows the effect of the observed early yielding on the elastic behavior at 0.5 M_u i.e. $\frac{\Delta_T}{\Delta_E} = 1.41$. The hybrid beams of Series 2 and 3 indicated that deflection considerations may be a limitation if 0.5 M_u is considered a reasonable working level. By comparing the $\frac{\Delta_T}{\Delta_E}$ ratios for beams 33a and 33b with this ratio for beam 23, it can be seen that the high strength steel portion of the web using ASTM A514 improved the elastic performance. For the beams with portions of the web using ASTM A441 steel, the difference in elastic performance was very small.

Effect of Anticlastic Curvature on the Ultimate Strength of Test Specimens

All specimens, except 13, 14a, 14b and 15, had one or more longitudinal cracks in the top of the slab. These cracks started in the maximum moment region, and in some specimens propagated out into the shear span as rotation increased. These cracks were due to the strains induced by the anticlastic curvature, an effect of Poisson's ratio, and were detected only at loads approaching the ultimate.

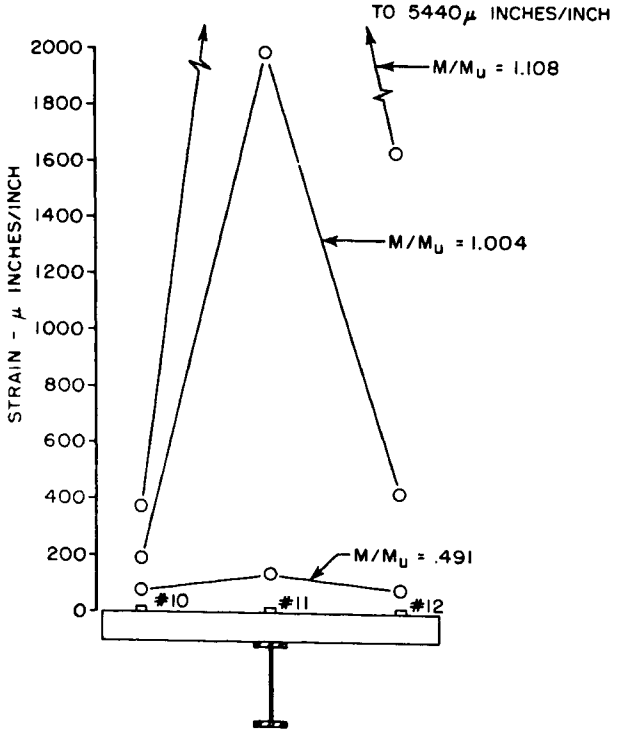

FIGURE 33 DISTRIBUTION OF TRANSVERSE STRAINS AT MIDSPAN FOR SPECIMEN 33b

This phenomenon which is particularly pronounced in the bending of plates, also occurs in the top flange of a transformed composite beam. The concrete flange is analogous to a simple plate stiffened at the centerline by the web and bottom flange. For this reason, the effect of anticlastic curvature is more apparent in T beams than in rectangular beams; although in theory, it exists in any beam subject to bending stresses. Since this curvature is directly related to bending curvature, it was quite noticeable in all beams which failed after considerable deflection and rotation. Figure 33 shows transverse tensile strains in the concrete measured with electric strain gages placed on the top of the concrete flange of beam 33b. It can be seen that strain usually associated with tension cracking of concrete occurred at a moment of approximately 0.5 M_u; however, cracks became visible only at 0.98M_u. This type of cracking apparently had negligible or no effect on the ultimate strength of the beams.

Strain Measurements

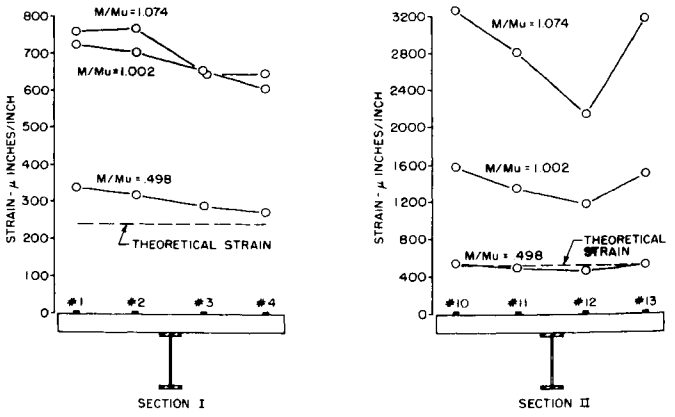

FIGURE 34 DISTRIBUTION OF LONGITUDINAL STRAINS IN SPECIMEN 32

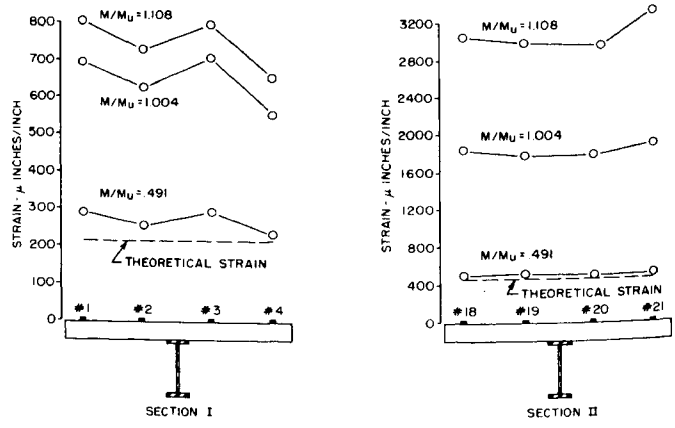

FIGURE 35 DISTRIBUTION OF LONGITUDINAL STRAINS IN SPECIMEN 33b

Longitudinal strains measured in the concrete of beams 32 and 33b are given in Figures 34 and 35. It can be seen at approximately M = 0.5M_u, the concrete strains at the top of the slab were uniform along the width of the specimen. However, at higher loads the strains vary from point to point in the same cross section, although the patterns of strain distribution established at low moments did not change at high values of moment.

NOMENCLATURE

a = depth of concrete stress block

b = width of concrete compression flange

C = total compressive force in the composite section

c' = compressive force in concrete flange of a composite beam with inadequate shear connectors

c'' = compressive force in the steel section of a composite beam with inadequate shear connectors

d = total depth of composite section

f_c' = cylinder strength of concrete at the age of testing

f_y = yield stress of steel

jd = moment arm between resultant compression and tension forces at M_u

M = moment measured at any time = 3.25 x P

M_m = maximum applied moment (includes dead load of 7.1 ft-kips)

M_p = theoretical plastic moment capacity of the steel section alone

M_{ps} = total theoretical ultimate resisting moment of the concrete slab and steel section acting together but without composite action

M_u = theoretical ultimate moment of a composite section with adequate shear connectors

M_u' = theoretical ultimate moment of a composite section with inadequate shear connectors

M_y = theoretical yield moment based on first yield at any point in the beam

P = externally applied load

P_y = externally applied load at M_y

q_u = the ultimate shear strength of a shear connector

T = total tensile force in the composite section

t = thickness of concrete flange

$\triangle_E$ = theoretical elastic centerline deflection at $0.5M_u$

$\triangle_T$ = measured centerline deflection at $0.5M_u$

ACKNOWLEDGEMENTS

This investigation was carried out under a research grant from the Committee of Steel Plate Producers of American Iron and Steel Institute and under the supervision of the Joint Engineering Subcommittee of the Committees of Structural Steel and Steel Plate Producers.

The authors take this opportunity to thank Dr. Ivan M. Viest for his continued interest in this project and for the technical guidance he provided in his capacity as project contact member of the Joint Engineering Subcommittee.

The investigation was carried out in the Materials Laboratory of the Department of Civil Engineering at The University of Texas. Appreciation is expressed to the staff of the laboratory and to the many graduate and undergraduate students who assisted in this project. Thanks are also due for the splendid cooperation and help given by the staff of the Bureau of Engineering Research, College of Engineering.

REFERENCES

1. *American Association of State Highway Officials* Standard Specifications for Highway Bridges, *7th Edition, Div. I, Sect. 9, 1957.*
2. *American Institute of Steel Construction* Specifications for the Design, Fabrication, and Erection of Structural Steel for Buildings, *New York, New York, 1963.*
3. *Joint ASCE-ACI Committee on Composite Construction* Tentative Recommendations for the Design and Construction of Composite Beams and Girders for Buildings, *Proceedings ASCE, Structural Division, December 1960, pp. 73-92.*
4. *Culver, C., Zarzeczny, P. J., Driscoll, G. C.* Composite Design for Buildings, *Progress Report No. 1, Fritz Engineering Laboratory Report No. 279.2, Lehigh University, January 1961*
5. *Culver, C., Zarzeczny, P. J., Driscoll, G. C.,* Composite Design for Buildings, *Progress Report No. 2, Fritz Engineering Report No. 279.6, Lehigh University, January 1961.*
6. *Viest, I. M., Fountain, R. S., Singleton, R. C.* Composite Construction in Steel and Concrete *McGraw-Hill Book Company, New York, 1958.*
7. *Toprac, A. A., Engler, R. A.* Plate Girders with High Strength Steel Flanges, and Carbon Steel Webs, *Proceedings, 1961 National Engineering Conference, American Institute of Steel Construction, New York, New York, pp. 83-94.*
8. *Slutter, R. G., Driscoll, G. C.* Composite Design for Buildings, *Progress Report No. 3, Fritz Engineering Laboratory Report No. 279.10, Lehigh University, January 1962.*
9. *American Concrete Institute* Building Code Requirements for Reinforced Concrete, *ACI 318-63.*
10. *Delameter, R. S.* Experimental Design for Short-Span Bridges, *Modern Steel Construction, American Institute of Steel Construction, New York, Vol. III, Num. 2/Second Quarter 1963, pp. 10-12.*
11. *Slutter, R. G., Driscoll, G. C.* The Flexural Strength of Steel and Concrete Composite Beams, *Fritz Engineering Laboratory Report No. 279.15, Lehigh University, March 1963.*

APPENDIX A

U.S. STEEL S-300 FLOOR PLATE*

DETAILS (HANDBOOK)

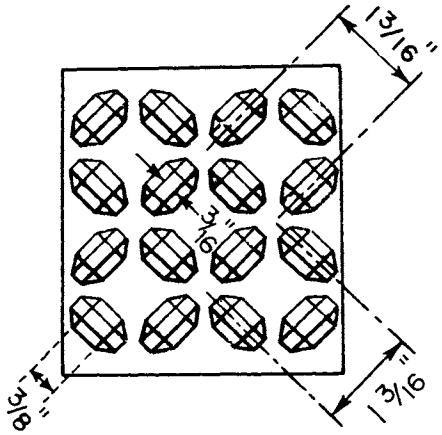

MEASURED DETAILS

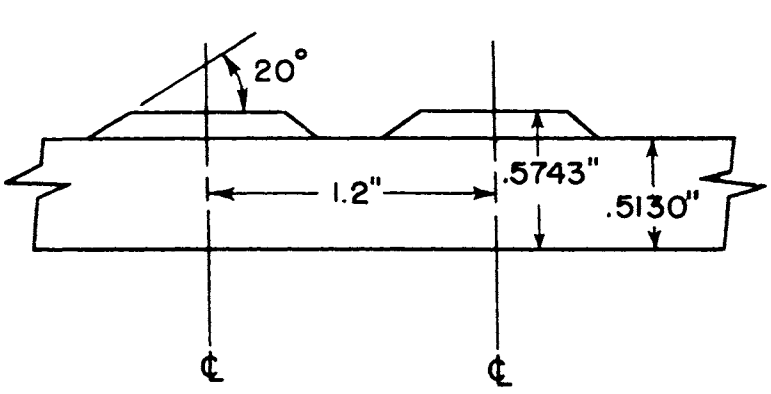

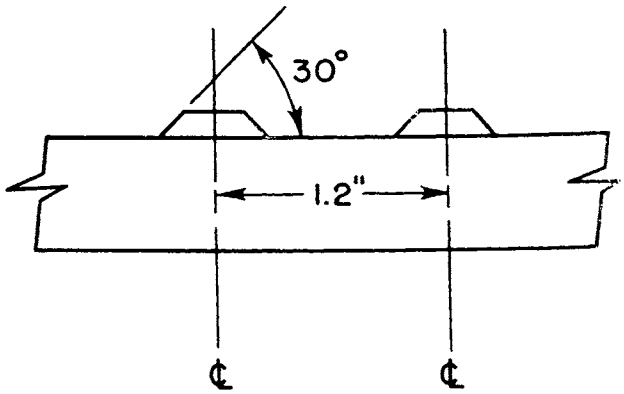

1. AREA OF DEFORMATIONS = 42% OF TOTAL
2. HEIGHT OF DEFORMATION = .574 - 0.513 = 0.061
3. ANGLE SHORT SIDE = 20° ±
   ANGLE LONG SIDE = 30° ±
4. DEFORMATIONS VERY IRREGULAR

---

*HOT ROLLED STEEL SHAPES AND PLATES
U.S. STEEL CORPORATION, MARCH 1962, p. 67

APPENDIX B

GREGORY INDUSTRIES, INC.
NELSON STUD WELDING DIVISION
LORAIN, OHIO 44055

CERTIFIED TEST REPORT

Date 12/2/63 Gregory Number HD-563 & HD-608 Customer Number 4159 & 4139

To: Central Texas Iron Works Co. Mail To: Dr. A. A. Toprac

21 st & Webster Avenue
Waco, Texas

c/o University of Texas
Engineering Department
Austin, Texas

Description of Material and Specifications:

1/2" x 3" H4F and 3/8" x 3" H4F Welding Studs. Material Furnished on these Purchase Orders conform to all specifications as are fully set forth therein.

MECHANICAL PROPERTIES AND TESTS

Tensile P. S. I.	70,000 Min.
Yield P. S. I.	60,000 Min.
% Elongation	20% Min.
% Reduction of area	

Other:

CHEMICAL ANALYSIS

Carbon	0.23% Max.
Manganese	0.60% Max.
Phosphorous	0.040% Max.
Sulphur	0.050% Max.

The above tests conform to the requirements of the specifications listed. We, hereby, certify that the foregoing data is a true copy of the data resulting from tests performed in Gregory Industries' Lab, and certified data furnished us by the producing mill.

State of Ohio: Lorain County:
Sworn to before me and signed in my presence,
This 2nd Day of December

Joseph A. Davoli
Notary Public
My commission expires: July 31, 1967

GREGORY INDUSTRIES, INC.

BY: _____
Authorized Agent

Shipped; 4/29 & 5/3/63.

APPENDIX C. MOMENT-DEFLEFLECTION CURVES

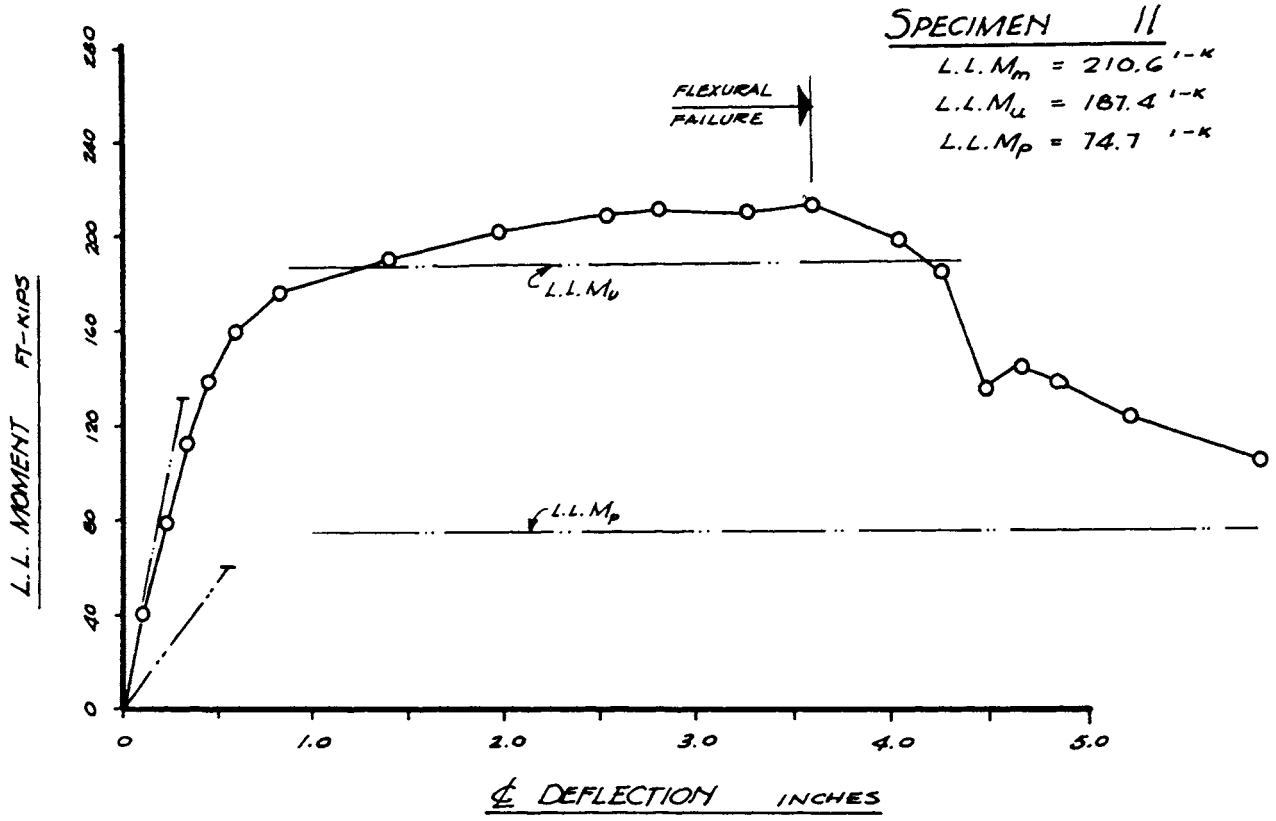

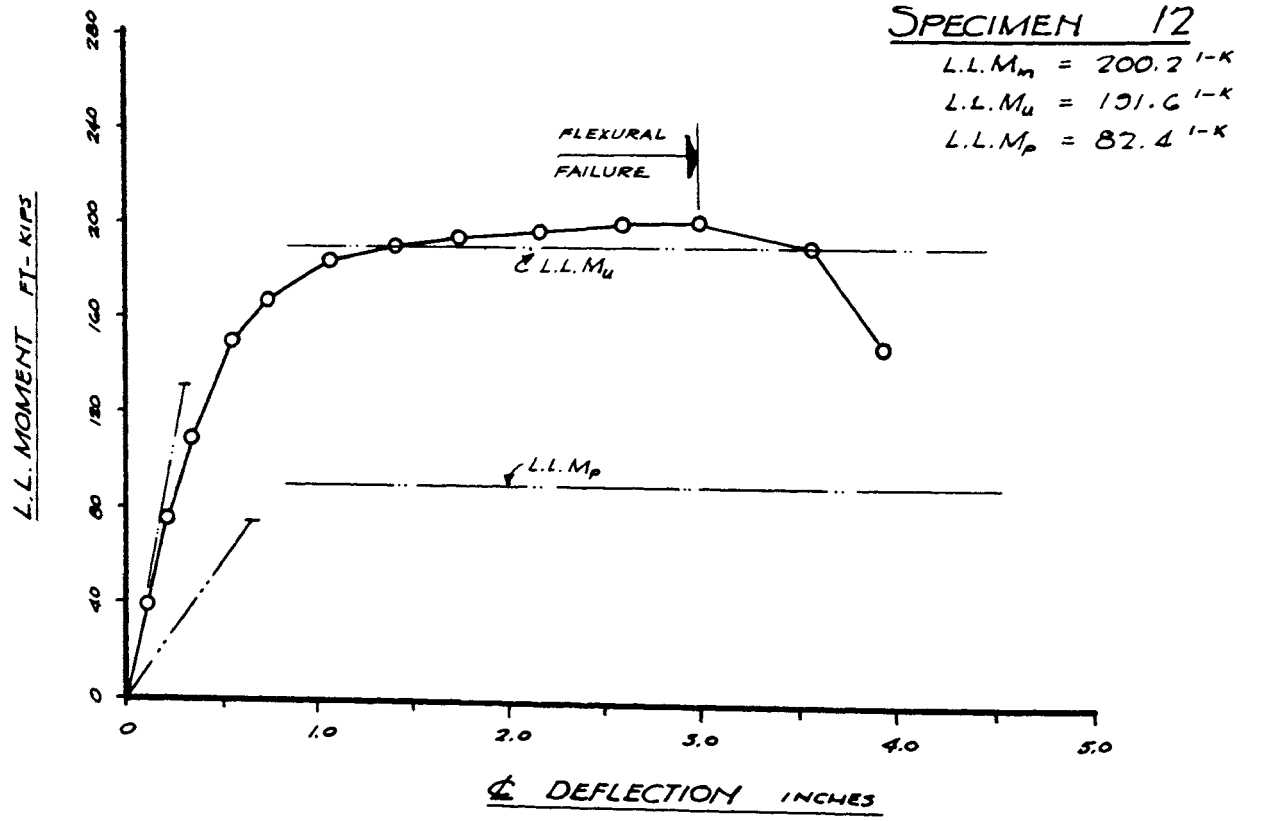

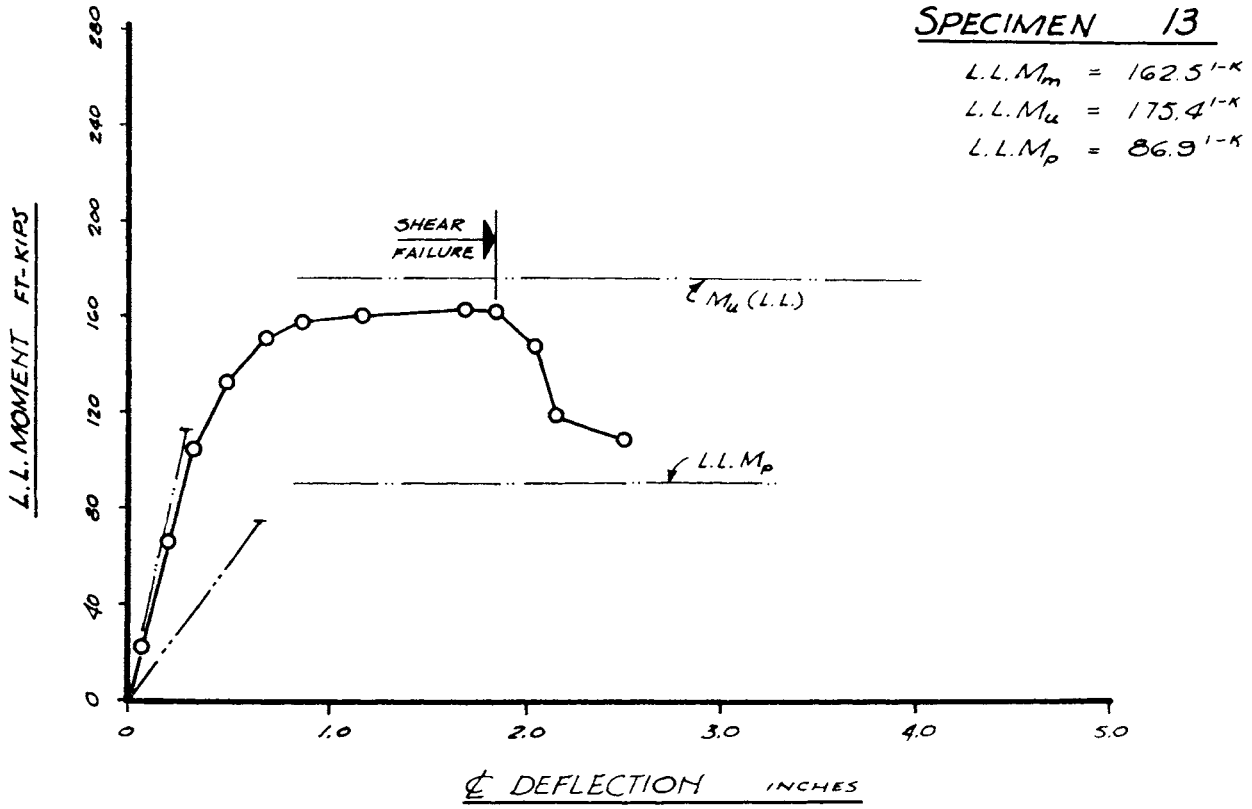
SPECIMEN 13
L.L. M_m = 162.5 I-K
L.L. M_u = 175.4 I-K
L.L. M_p = 86.9 I-K
L.L. MOMENT FT-KIPS
0
40
80
120
160
200
240
280
SHEAR FAILURE
℄ M_u (L.L.)
℄ L.L. M_p
0
1.0
2.0
3.0
4.0
5.0
℄ DEFLECTION INCHES

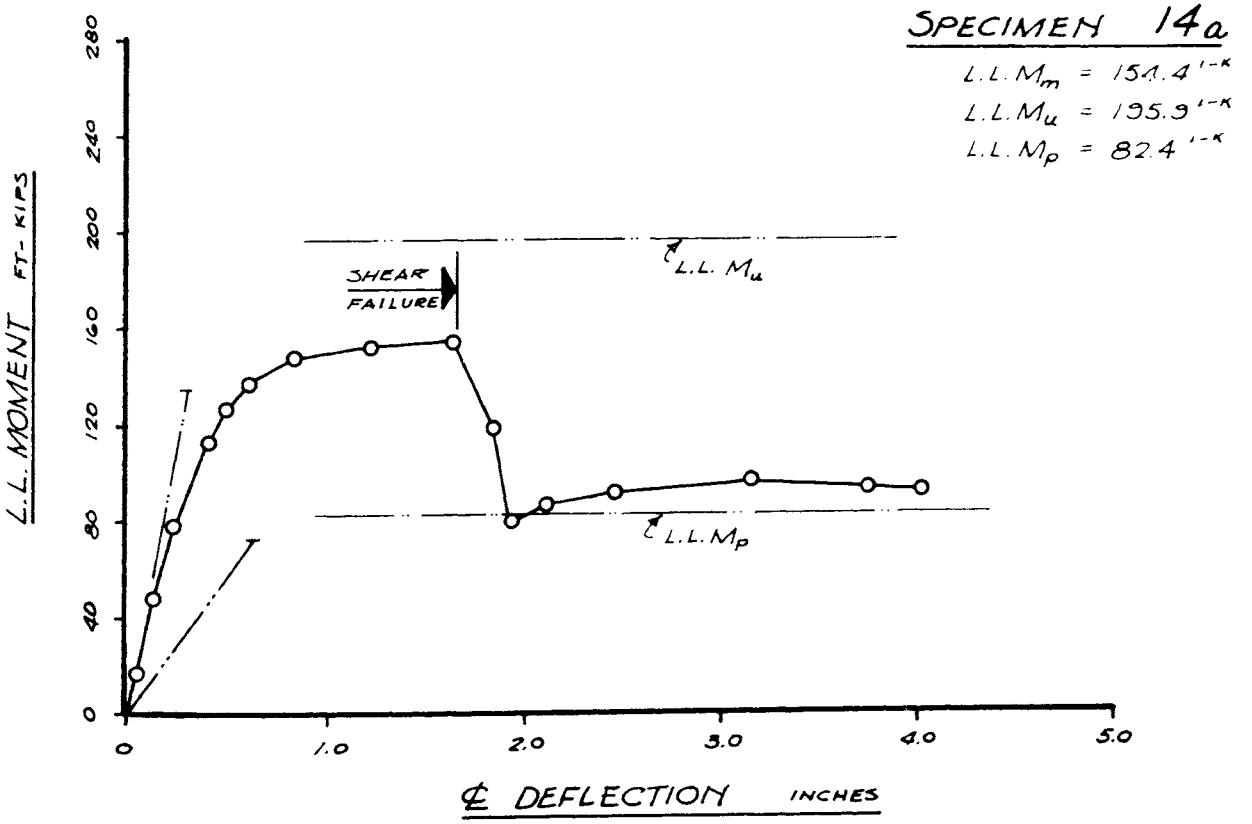
SPECIMEN 14a
L.L. M_m = 151.4 I-K
L.L. M_u = 195.9 I-K
L.L. M_p = 82.4 I-K
L.L. MOMENT FT-KIPS
0
40
80
120
160
200
240
280
SHEAR FAILURE
℄ L.L. M_u
℄ L.L. M_p
0
1.0
2.0
3.0
4.0
5.0
℄ DEFLECTION INCHES

SPECIMEN 14b

L.L. M_m = 165.1 ft-k

L.L. M_u = 191.1 ft-k

L.L. M_p = 82.4 ft-k

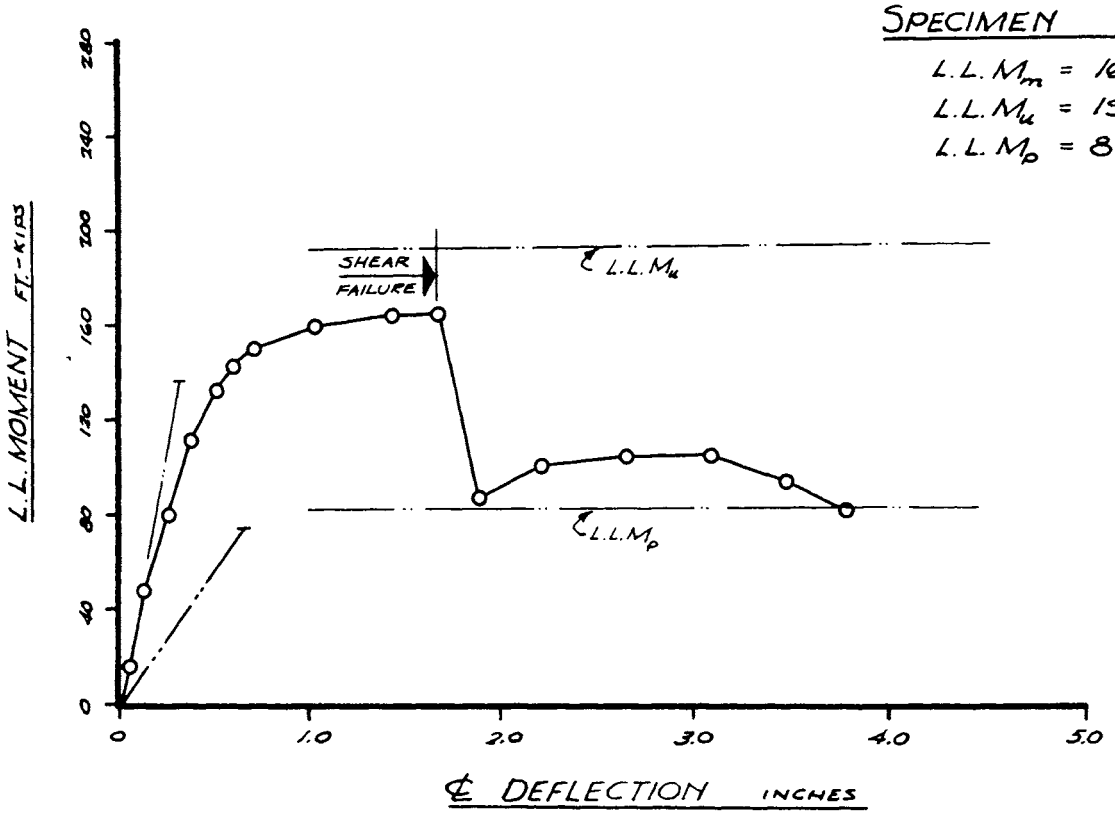

SPECIMEN 15

L.L. M_u = 132.0 ft-k

L.L. M_u = 190.9 ft-k

L.L. M_p = 82.4 ft-k

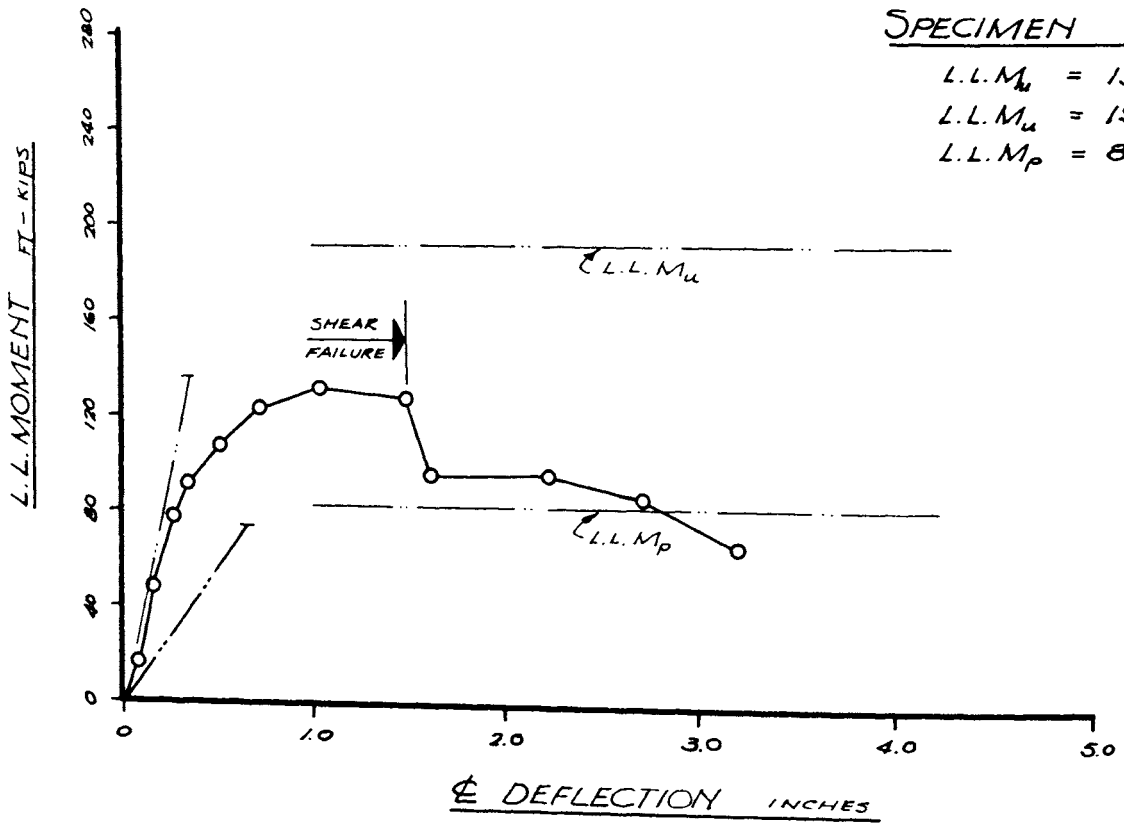

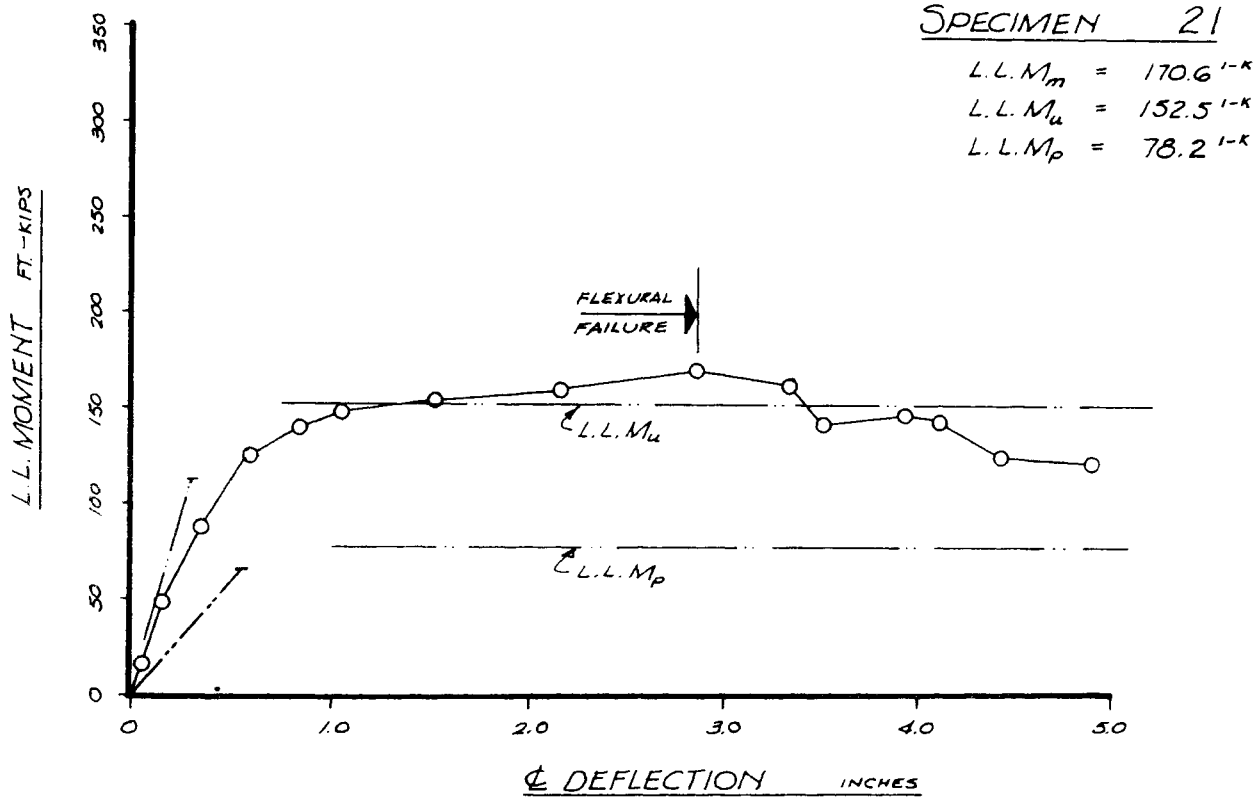
SPECIMEN 21
L.L.M_m = 170.6 ft-k
L.L.M_u = 152.5 ft-k
L.L.M_p = 78.2 ft-k
FLEXURAL FAILURE
$\mathcal{L}$ L.L.M_u
$\mathcal{L}$ L.L.M_p
L.L. MOMENT FT.-KIPS
0
50
100
150
200
250
300
350
0
1.0
2.0
3.0
4.0
5.0
℄ DEFLECTION INCHES

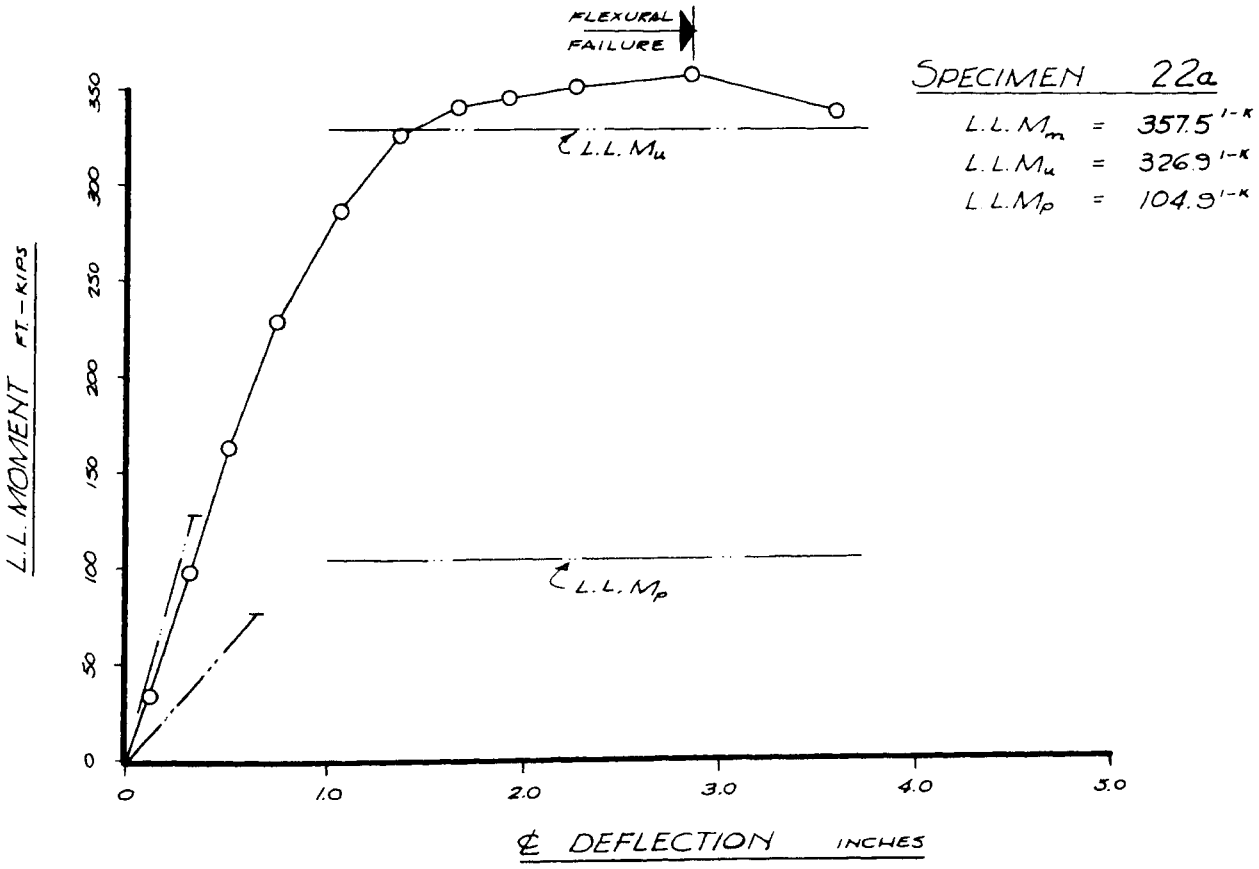
FLEXURAL FAILURE
SPECIMEN 22a
L.L.M_m = 357.5 ft-k
L.L.M_u = 326.9 ft-k
L.L.M_p = 104.9 ft-k
$\mathcal{L}$ L.L.M_u
$\mathcal{L}$ L.L.M_p
L.L. MOMENT FT.-KIPS
0
50
100
150
200
250
300
350
0
1.0
2.0
3.0
4.0
5.0
℄ DEFLECTION INCHES

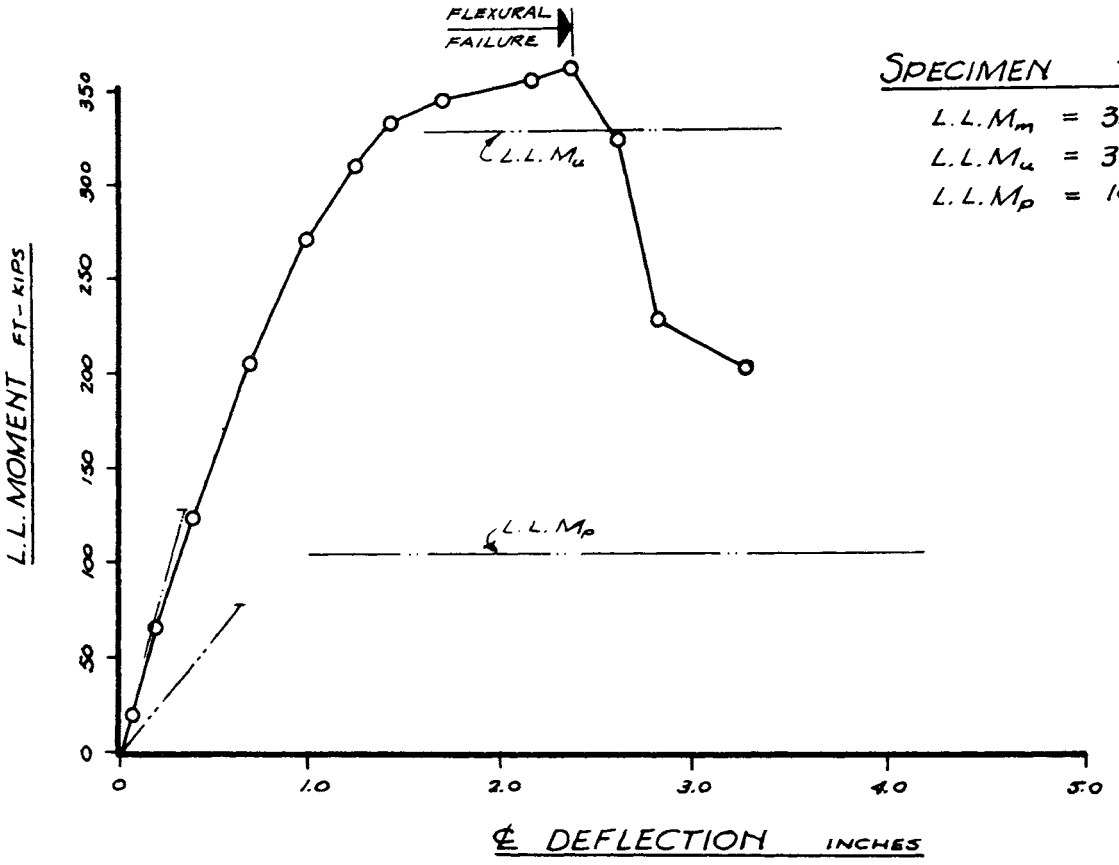

SPECIMEN 22b

L.L. M_m = 357.5 ft-k

L.L. M_u = 326.9 ft-k

L.L. M_p = 104.9 ft-k

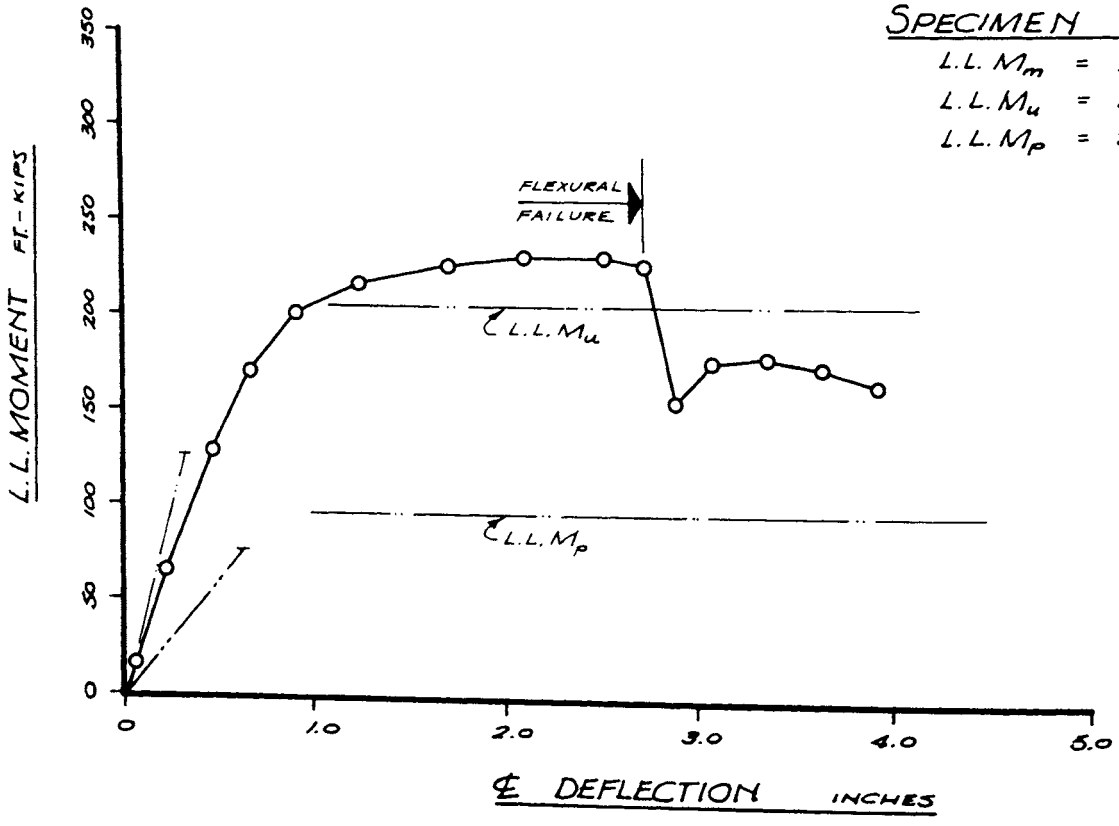

SPECIMEN 23

L.L. M_m = 237.2 ft-k

L.L. M_u = 204.9 ft-k

L.L. M_p = 95.9 ft-k

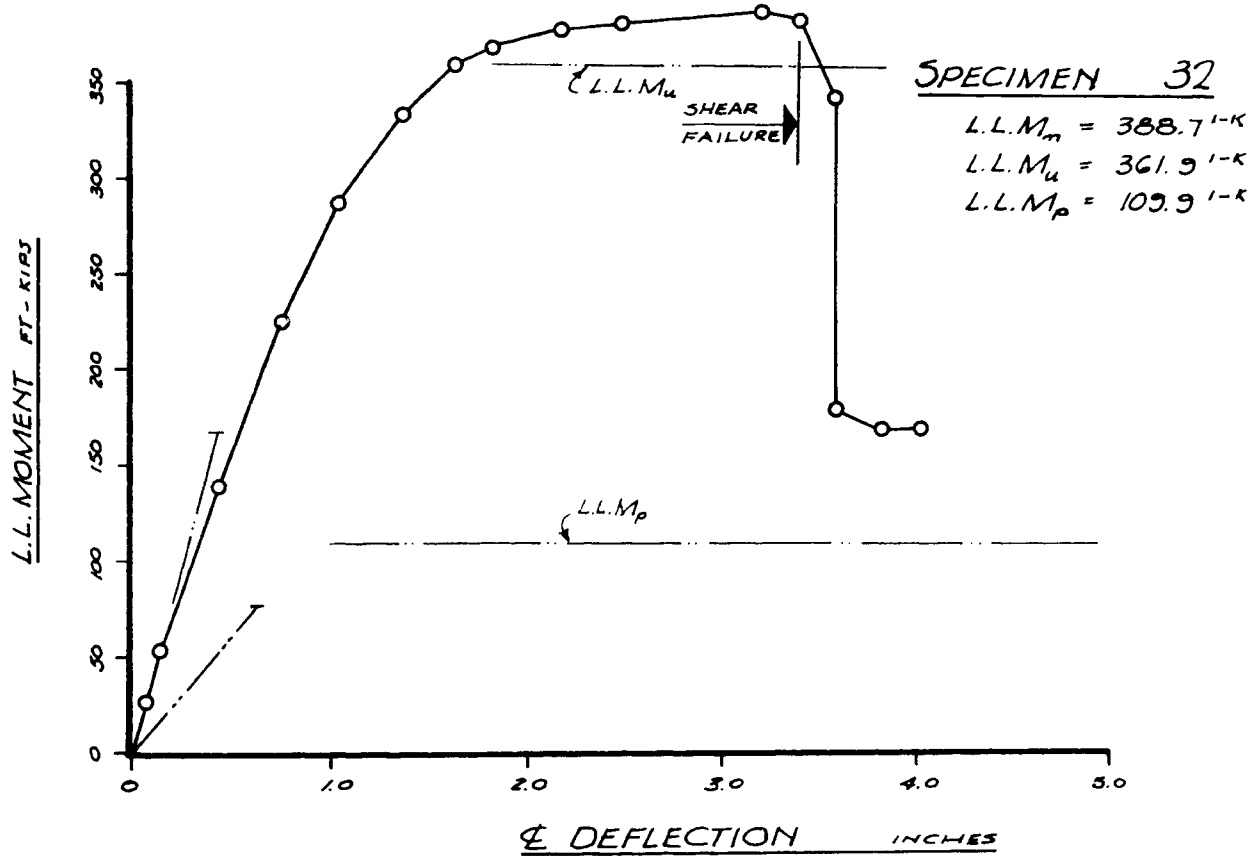
SPECIMEN 32
L.L.M_m = 388.7 ft-k
L.L.M_u = 361.9 ft-k
L.L.M_p = 109.9 ft-k
L.L.M_u
SHEAR FAILURE
L.L.M_p
L.L. MOMENT FT-KIPS
0
50
100
150
200
250
300
350
1.0
2.0
3.0
4.0
5.0
℄ DEFLECTION INCHES

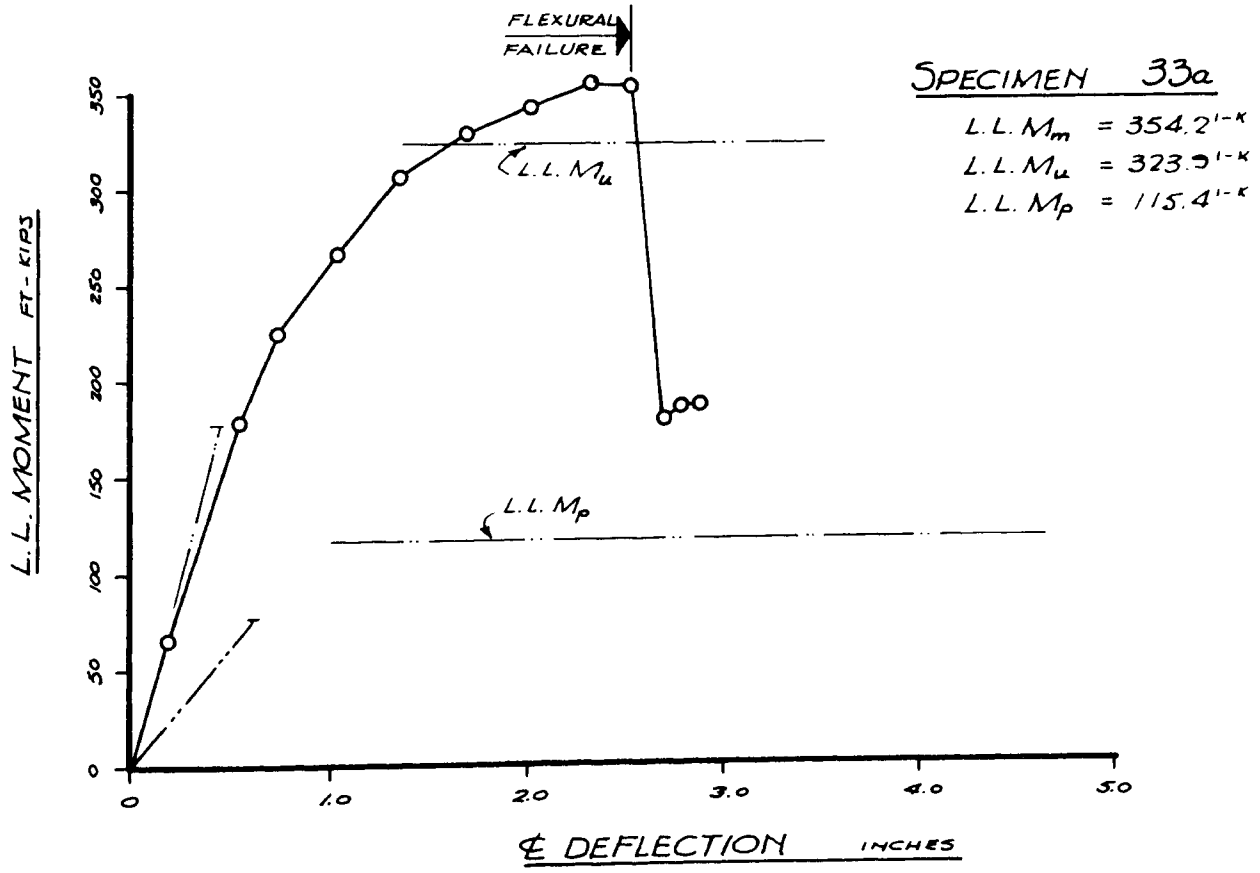
SPECIMEN 33a
L.L.M_m = 354.2 ft-k
L.L.M_u = 323.3 ft-k
L.L.M_p = 115.4 ft-k
FLEXURAL FAILURE
L.L.M_u
L.L.M_p
L.L. MOMENT FT-KIPS
0
50
100
150
200
250
300
350
1.0
2.0
3.0
4.0
5.0
℄ DEFLECTION INCHES

APPENDIX C. (CONT.)

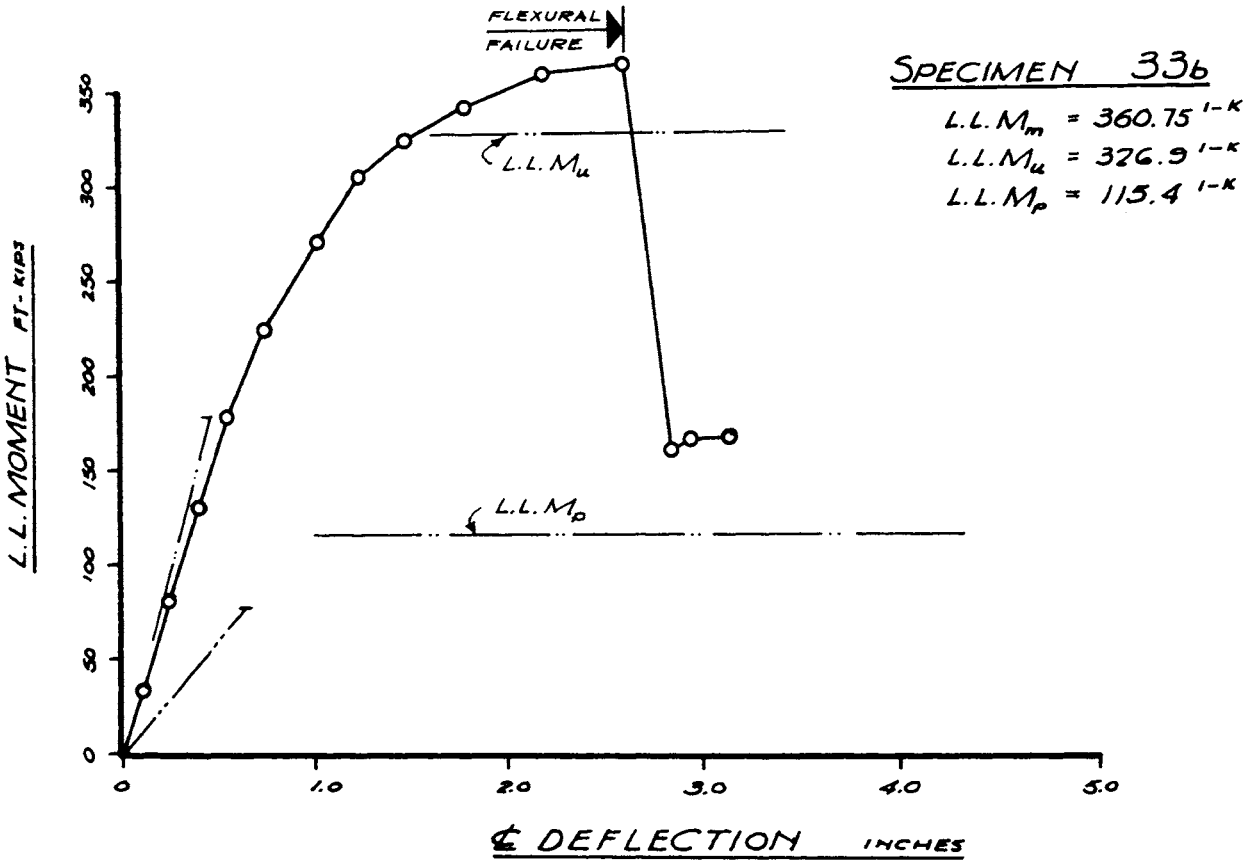

SPECIMEN 33b

L.L. M_m = 360.75 $^{1-K}$

L.L. M_u = 326.9 $^{1-K}$

L.L. M_p = 115.4 $^{1-K}$

APPENDIX C. (CONT.)

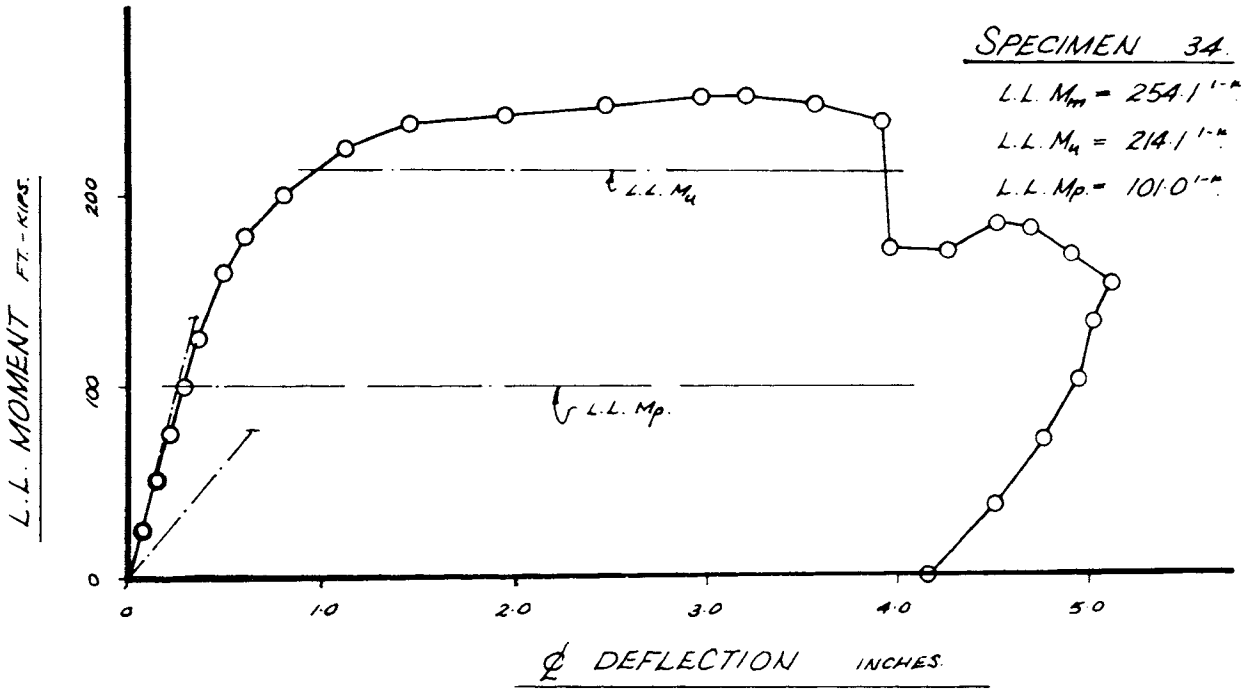

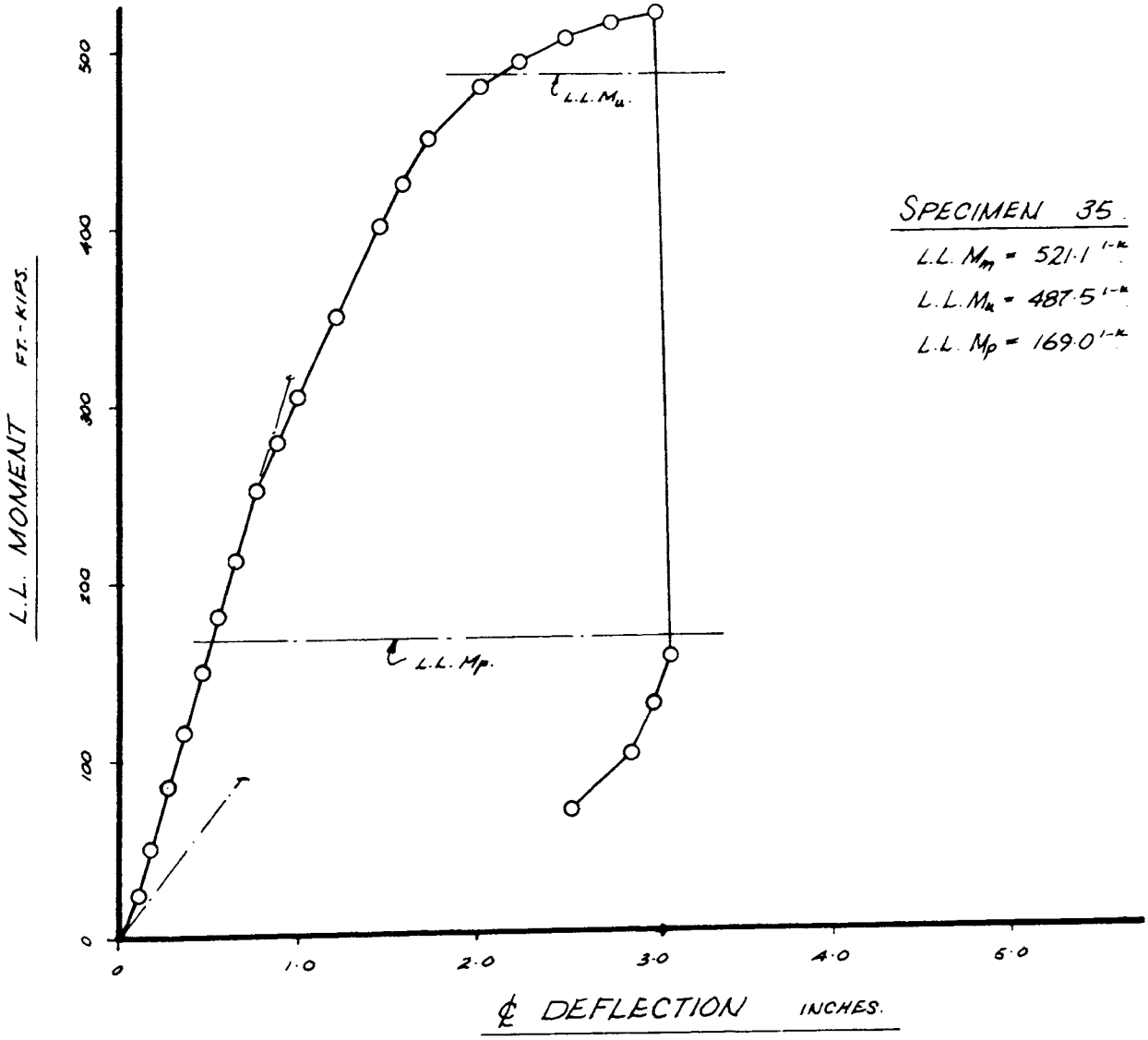

SPECIMEN 41a

$L.L.M_m = 244.4^{I-K}$
$L.L.M_u = 221.9^{I-K}$
$L.L.M_p = 65.2^{I-K}$

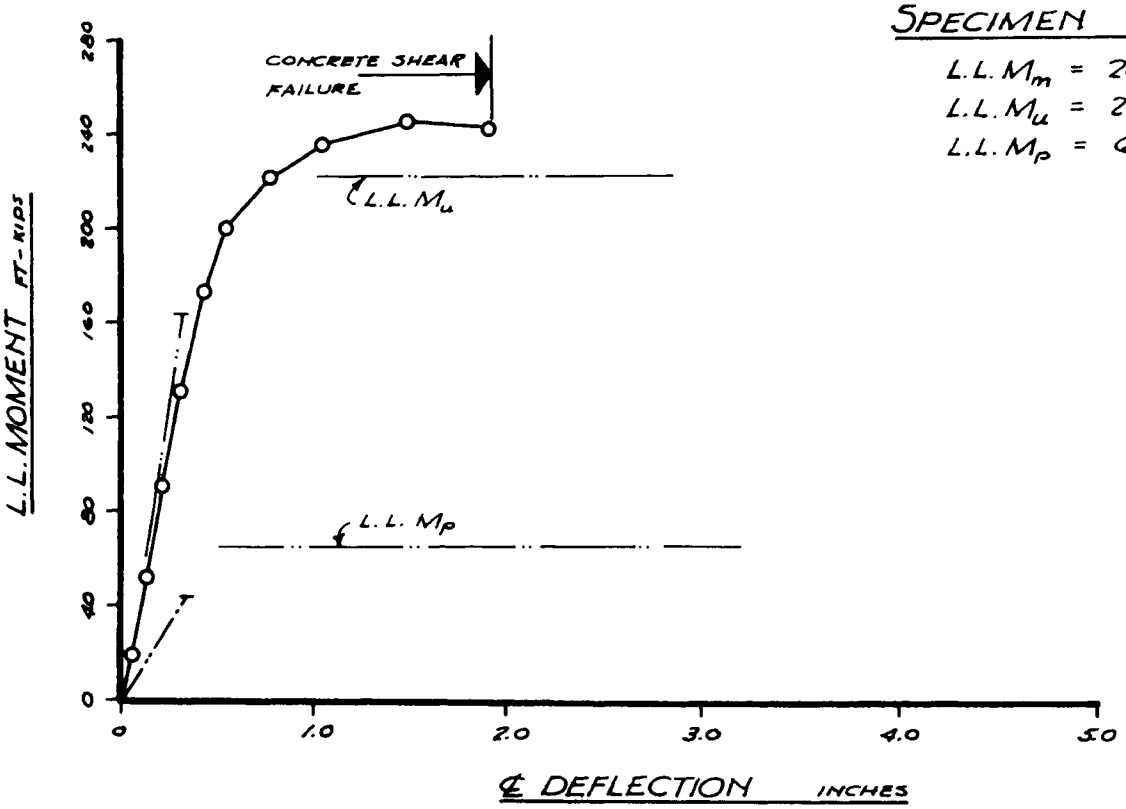

SPECIMEN 41b

$L.L.M_m = 227.5^{I-K}$
$L.L.M_u = 206.5^{I-K}$
$L.L.M_p = 65.2^{I-K}$

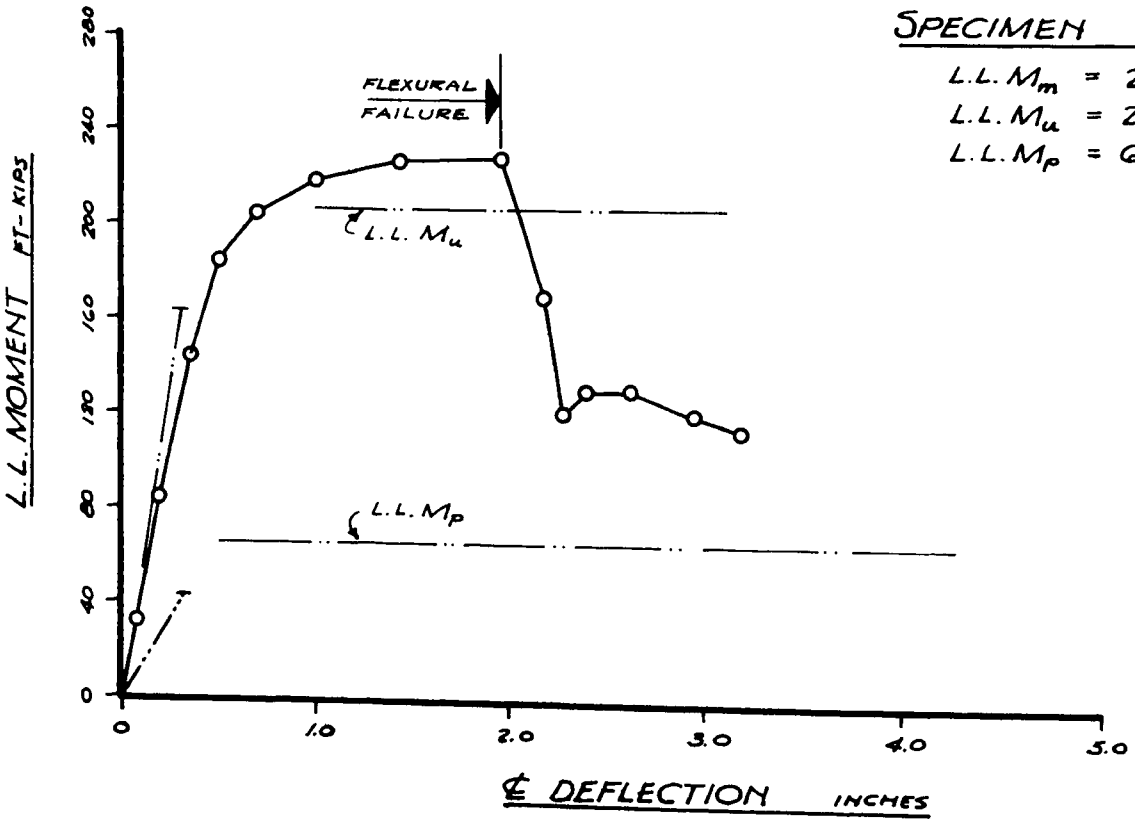

Beam Number	M ft-kips	M/M_u	Remarks
11	52.0	.277	Slipping noise from west shear span.
	126.1	.673	Yield lines appear in web.
	138.3	.738	Cracking sounds from west shear span.
	182.0	.970	Visible cracks appear in edge of slab and yield line extend to within 2½" of top flange.
	190.5	1.016	Cracks opening up in bottom of concrete slab.
	199.8	1.065	Longitudinal crack visible about ⅓ of shear span starting under the load.
	209.6	1.118	Crushing of concrete beginning.
	210.6	1.122	Crushing complete, plastic hinge formed after considerable deformation.
	143.0	.763	Compression yield lines forming in top flange of steel section.
	105.6	.563	Steel beam failed by web buckling. Test stopped.
12	74.1	.387	Loud noises from shear spans.
	108.7	.567	Hairline cracking of concrete in constant moment section.
	195.6	1.021	Cracking noises.
	199.9	1.042	Slippage at east end with separation of slab from steel section.
	200.2	1.046	Steel section plastic in tension at constant moment section. Concrete starting to crush.
	192.4	1.005	Pure hinge action.
	149.5	.780	Compression yield lines fully developed. Whole section buckled laterally to south. Test stopped.
13	109.2	.623	Yield lines appear in web next to weld.
	121.5	.693	First yield lines on bottom flange.
	158.6	.903	Cracking in concrete slab beginning.
	161.2	.918	Yield lines forming in compression flange.
	146.3	.833	Load cracking noise as load fell off sharply.
	118.3	.674	Further cracking of concrete accompanied by loud noises. Extensive yield lines formed in compression flange and web of west span. Separation of beam and slab in each span.
	108.5	.618	West slab separated greatly and a large transverse crack opened with a loud cracking sound. Stopped test.
14a	48.7	.249	Loud pop in east shear span close to load.
	89.7	.458	First yield lines in web close to weld.
	146.2	.747	First yield lines in bottom flange.
	150.8	.768	First visible cracks in underside of slab. Yield lines up to mid depth of steel section.
	117.6	.600	Dull thud from near midspan towards west end. Compression yield lines and hinge forming under west load.
	91.0	.464	Test ended due to web buckling of steel section.

Appendix D. Synopsis Of Beam Behavior—*Continued*

Beam Number	M ft-kips	M/M_u	Remarks
14b	65.0	.341	Loud noises from near the load in the east shear span.
	97.5	.511	First small yield lines in web close to weld.
	132.6	.694	First visible cracks in slab. Yield lines advancing.
	149.5	.783	First yield lines in bottom flange.
	164.1	.858	Compression yield lines beginning in top flange.
	87.7	.460	Large crack opened under the east load accompanied by the formation of extensive compression yield lines. East shear span separated from steel section.
	104.6	.547	Steel section beginning to slide towards the north.
	81.2	.425	Local buckling under east load brought test to end.
15	78.0	.408	Loud noises from shear spans.
	100.7	.527	First yield lines in bottom flange.
	108.9	.570	First observation of cracking in concrete.
	128.4	.673	Loud pop from east shear span.
	129.3	.676	Compression yield lines formed in flange and down into web, concentrated under east load.
	94.2	.493	Yield lines and flexural cracks forming well out into east shear span.
	96.8	.507	Extensive web buckling.
	92.3	.483	Steel section sliding across bottom of concrete slab.
	66.3	.347	Test stopped due to excessive lateral buckling of steel section.
21	61.7	.405	Loud cracking noise from east shear span.
	87.7	.575	Yield lines forming in web close to weld.
	100.7	.660	First yield lines in bottom flange.
	152.1	.996	First visible cracks in concrete slab with yield lines extending to within about 1½″ of top of steel section.
	164.1	1.077	Longitudinal crack extending out about two feet into each shear span.
	165.7	1.087	Crushing of concrete slab began.
	141.7	.930	Final crushing of the concrete slab occurred enroute to this load.
	147.9	.970	Steel section began to buckle.
	124.8	.818	Formation of first compression yield lines in top flange.
	122.8	.805	Test stopped due to excessive buckling.
22a	32.5	.101	Loud cracking noises from shear span.
	74.7	.232	Yield lines appearing in the web close to the weld.
	325.0	1.010	Compression yield lines appearing in the top flange along with tensile cracking in the concrete slab.
	351.0	1.091	Tensile yield lines appearing in the bottom flange.
	338.0	1.050	Complete crushing of concrete slab.

Appendix D. Synopsis Of Beam Behavior—*Continued*

Beam Number	M ft-kips	M/M_u	Remarks
22b	65.0	.194	Loud cracking noise from east shear span.
	97.5	.291	First yield lines appear in web close to weld.
	252.8	.754	Extensive yield lines forming in web.
	280.8	.838	Yield lines forming in top flange.
	308.7	.922	Tensile cracking in slab stabilized and longitudinal crack out to about ½ of each shear span.
	342.2	1.021	Longitudinal crack full length of east shear span.
	347.7	1.038	Yield lines appearing in bottom flange.
	357.5	1.067	Yield lines from the top flange crossing the tension yield lines from the bottom. Crushing beginning.
	226.2	.675	Crushing of the concrete slab progressing all across width, followed by formation of compression yield lines.
	200.2	.597	Beam rotated and steel section failed by buckling. Test was stopped.
23	65.0	.324	Loud cracking noises from shear span.
	127.7	.637	Yield lines beginning in web.
	216.8	1.081	Yielding in bottom flange beginning.
	230.7	1.150	Crushing in top of concrete slab starting.
	154.7	.772	Crushing of slab complete.
	176.8	.882	Compression yield lines beginning.
	172.2	.859	Top flange completely yielded.
	164.4	.820	Test ended due to lateral buckling causing beam to bear against machine columns.
32	104.2	.287	Cracking noise from midspan.
	188.5	.521	Yield lines appearing in web close to bottom weld.
	271.1	.748	First visible cracks in concrete slab.
	279.5	.772	Yield lines visible at intersection of upper and lower web.
	344.5	.952	Extensive yield lines forming in upper web only.
	351.0	.970	A few yield lines forming in top flange, probably at locations of studs. Longitudinal crack very conspicuous.
	365.3	1.010	First yield lines in bottom web.
	379.6	1.050	First visible yield lines in bottom flange.
	388.7	1.074	Formation of extensive yield lines in web and bottom flange accompanied by first signs of crushing in slab.
	344.5	.953	Crushing of concrete slab still limited.
	180.7	.517	Shear failure of studs in east shear span accompanied by formation of compression yield lines under the east load.
	169.0	.467	Test stopped due to severe buckling.

Appendix D. Synopsis Of Beam Behavior—*Continued*

Beam Number	M ft-kips	M/M_u	Remarks
33a	65.0	.196	Popping noises from shear span.
	253.5	.766	First evidence of yield lines in bottom flange and in A36 web just above the weld.
	279.5	.845	First visible cracking in concrete.
	342.9	1.036	Longitudinal crack visible in both shear spans.
	352.3	1.065	Yield lines up to bottom of top flange. First evidence of crushing observed.
	177.5	.536	Complete crushing of concrete slab.
	185.2	.560	Test terminated due to excessive buckling with complete yielding of top flange of steel section.
33b	97.5	.298	Cracking noise from east shear span.
	269.7	.818	First appearance of yield lines in bottom flange.
	321.7	.983	First visible cracks in concrete slab.
	347.7	1.063	Some yield lines in upper web and extensive yield lines in bottom flange.
	357.5	1.092	First observation of longitudinal crack.
	159.2	.487	Flexural failure occurred suddenly with crushing extending completely across concrete slab. Crushing was followed immediately by lateral buckling.
34	88.6	.41	Noise due probably to slip.
	153.3	.72	Yield lines observed in the A36 web.
	218.4	1.02	Yield lines in A441 flange.
	234.6	1.09	Yield lines in the A36 web developed to within 1½″ of top steel flange. The lower face of the concrete slab in the constant moment region cracked in 5 places.
	243.1	1.13	Yield lines reach top flange. The whole steel section, including A441, has yielded.
	245.6	1.14	Concrete tension cracks opened up further.
	254.1	1.185	Specimen refuses to carry larger load. Concrete compression failure under one of the load points and also at the south edge of the slab between load points.
	241.1	1.125	Concrete pieces fell off the slab.
	186.1	.87	Buckling to the north of the steel beam started.
	183.8	.86	Web buckled.

Appendix D. Synopsis Of Beam Behavior—*Continued*

Beam Number	M ft-kips	M/M_u	Remarks
35	330.0	.675	Slight relaxation in load has been observed.
	350.0	.718	Yield lines in the A36 web developed.
	400.0	.820	A36 web and flange (top) have yielded.
	462.0	.946	Concrete slab developed longitudinal crack extending from bearing to bearing.
	466.0	.958	Shear yielding in the A36 web.
	521.1	1.070	Sudden failure in concrete. Failure suggests that the whole concrete slab was in compression. Web and flange in the constant moment region buckled.
41a	243.1	1.095	First cracking observed in bottom of concrete slab.
	244.4	1.100	First observation of longitudinal crack along the centerline of the slab.
	241.8	1.090	Diagonal cracks observed in top of slab at roughly 45° to the centerline.
	198.3	.894	Diagonal cracks opened up considerably and beam refused additional load.
41b	172.9	.832	Longitudinal shrinkage crack began to open up. Crack was visible before loading.
	204.7	.984	First yield lines in bottom flange and beginning of yield lines in web.
	220.3	1.060	First visible tension crack in slab with yield lines up about 9″ from bottom.
	227.5	1.095	Beginning of a diagonal crack in slab under the west load.
	227.5	1.095	Further development of diagonal cracks with steel section completely yielded.
	206.7	.993	Beginning of crushing in concrete.
	120.2	.578	Complete crushing — flexural failure.
	130.0	.625	Compression yield lines forming in top flange of steel section.
	130.0	.625	Steel web stabbing through the slab at the centerline.
	115.7	.556	Test stopped due to excessive lateral buckling of beam.

american iron and steel institute

150 East 42nd Street, New York, N. Y. 10017